Origins of the nitrate ^{15}N depletion in the Mediterranean Sea

Tanja Wald[1,2], F Fripiat[3], A D Foreman[1], T Tanhua[4], G Sisma-Ventura[5], Y Ryu[6], D Marconi[6], D M Sigman[6], G H Haug[1,2], and Alfredo Martínez-García[1]

[1]Max Planck Institute for Chemistry
[2]ETH Zürich
[3]Department of Geosciences, Environment and Society, Université Libre de Bruxelles
[4]GEOMAR Helmholtz Centre for Ocean research Kiel
[5]Israel Oceanographic and Limnological Research Institute
[6]Department of Geosciences, Princeton University

January 29, 2024

Origins of the nitrate ^{15}N depletion in the Mediterranean Sea

T. Wald[*1,2], F. Fripiat[3], A.D. Foreman[1], T. Tanhua[4], G. Sisma-Ventura[5], Y. Ryu[6], D. Marconi[6], D.M. Sigman[6], G.H. Haug[1,2], and A. Martínez-García[*1]

[1]Max Planck Institute for Chemistry, Mainz, Germany.

[2]ETH Zürich, Zürich, Switzerland.

[3]Department of Geosciences, Environment and Society, Université Libre de Bruxelles, Bruxelles, Belgium.

[4]GEOMAR Helmholtz Centre for Ocean research Kiel, Kiel, Germany.

[5]Israel Oceanographic and Limnological Research Institute, Haifa, Israel.

[6]Department of Geosciences, Princeton University, Princeton, NJ, USA.

[*]Corresponding author: Tanja Wald (Tanja.Wald@mpic.de) and Alfredo Martínez-García (a.martinez-garcia@mpic.de).

Key Points:

- Basin-wide depth profiles of nitrate δ^{15}N and δ^{18}O support an external supply of low-δ^{15}N N into the Mediterranean Sea.
- Nitrate δ^{15}N can be explained by modest rates of N_2 fixation, anthropogenic N deposition, and/or partial breakdown of dissolved organic N.
- The ^{15}N-depleted input is best expressed in the eastern basin due to isolation from the Atlantic nitrate inflow.

Abstract

This study presents basin-wide, full-depth profiles of nitrate δ^{15}N (*vs.* Air) and δ^{18}O (*vs.* Vienna Standard Mean Ocean Water, VSMOW) in the Mediterranean Sea, based on seawater samples collected during three separate cruises: the TalPro cruise in summer 2016, the MSM72 cruise in spring 2018, and the HaiSec45 cruise in spring 2021. Our results reveal a consistent ^{15}N depletion across the entire Mediterranean Sea in comparison to the global ocean, with significantly lower nitrate δ^{15}N values in the eastern basin (2.2 ± 0.2‰) than in the western basin (2.9 ± 0.1‰). In contrast, there is no significant difference in nitrate δ^{18}O between the two basins (2.2 ± 0.3‰ and 2.1 ± 0.2‰, respectively). These observations point to an external supply of low-δ^{15}N N (ultimately, nitrate) to the Mediterranean Sea. This supply is gradually diluted by the Atlantic nitrate inflow, thus creating an east-to-west gradient in nitrate δ^{15}N. Earlier studies have attributed this external low-δ^{15}N N supply to either N_2 fixation or atmospheric deposition of anthropogenic N. A prognostic four-box model reveals that given the 120 – 170-year residence time of water in the Mediterranean Sea, modest rates of these sources, individually or in combination, can account for the observed low δ^{15}N values. Additionally, we identify partial degradation of dissolved organic nitrogen, introduced into the Mediterranean Sea from the Atlantic Ocean, as another possible source of low-δ^{15}N nitrate. Distinguishing among these sources will require reconstruction of Mediterranean nitrate δ^{15}N through time, using paleoceanographic proxies.

1 Introduction

The Mediterranean Sea is the largest semi-enclosed marine basin. It is characterized by an anti-estuarine circulation in which the Atlantic surface water inflow (AW) via the Strait of Gibraltar is modified through evaporation on its way to the east, leading to the formation of new intermediate (Levantine Intermediate Water, LIW) and deep waters that are ultimately exported as Mediterranean Outflow Water to the Atlantic Ocean (Schneider et al., 2014). The anti-estuarine circulation gives rise to pronounced oligotrophic conditions in the western Mediterranean basin, which reaches ultraoligotrophic conditions in the eastern Mediterranean basin (Bethoux, 1989; Pujo-Pay et al., 2011). This is attributed to the import of surface waters from the Atlantic Ocean and the export of more nutrient-rich waters at depth (Krom et al., 2010; Powley et al., 2017).

Measurements of nitrate $\delta^{15}N$ have revealed low $\delta^{15}N$ values (i.e., 2 – 3‰ (*vs.* Air)) in the deep Mediterranean Sea (Emeis et al., 2010; Pantoja et al., 2002) compared to other deep waters, which typically have a nitrate $\delta^{15}N$ value of 4.6‰ or higher (Sigman et al., 2000, 2009). Different authors have attributed the low nitrate $\delta^{15}N$ values in the Mediterranean Sea to one of two processes: N_2 fixation (e.g., Pantoja et al., 2002; Sachs and Repeta, 1999) or anthropogenic inputs (e.g., Emeis et al., 2010; Krom et al., 2004). N_2 fixation describes the biological conversion of atmospheric N_2 to fixed N by diazotrophs and introduces nitrate to the ocean interior with a $\delta^{15}N$ of ~ −1‰ largely through export production of organic nitrogen (N) and its remineralization (Carpenter et al., 1997; McRose et al., 2019; Minagawa & Wada, 1986). Anthropogenic input consists of river discharge and atmospheric deposition. River discharge into the Mediterranean Sea does appear to add a substantial amount of N into the Mediterranean Sea, but this N has expected to have a high nitrate $\delta^{15}N$ (~ 8 – 12‰, Johannsen et al., 2008; Mayer et al., 2002) that cannot explain the low nitrate $\delta^{15}N$ of the Mediterranean interior waters. In contrast, atmospheric deposition, both wet and dry, shows consistently negative $\delta^{15}N$ values for nitrate deposition (i.e., weighted annual average of −3.1‰; Mara et al., 2009), making it a plausible candidate for reducing nitrate $\delta^{15}N$ of the Mediterranean Sea.

The anomalously high nitrate-to-phosphate (N:P) ratio in intermediate and deep Mediterranean waters is considered as a supporting argument for a N-dominated nutrient source to the Mediterranean Sea, consistent with either N_2 fixation or anthropogenic deposition (e.g., Krom et al., 2010; Pantoja et al., 2002; Powley et al., 2014; Sachs & Repeta, 1999). In the western basin, the N:P ratio is 23:1, increasing to 28:1 in the eastern basin (Béthoux et al., 1998; Kress & Herut, 2001; Krom et al., 1991, 2005; Pujo-Pay et al., 2011; Ribera d’Alcalà et al., 2003), much higher than the Redfield ratio of 16:1 (Redfield et al., 1963).

In this study, we present nitrate $\delta^{15}N$ and $\delta^{18}O$ depth sections across all basins of the Mediterranean Sea. This dataset is used to investigate the origins of the low nitrate $\delta^{15}N$ in the Mediterranean Sea. To aid in this effort, a prognostic four-box model of fixed N and its isotopes is developed and applied.

2 Materials and Methods

2.1 Sampling

Seawater samples were collected during the TalPro cruise in August 2016 as part of the MedSHIP-program (Mediterranean ship-based hydrographic investigations program), the MSM72 cruise in March – April 2018 contributing to the global repeat hydrography program GOSHIP, and the HaiSec45 cruise in March 2021 (Figure 1). The TalPro cruise with R/V *Angeles Alvariño* included two transects with 33 stations sampled for nitrate δ^{15}N and δ^{18}O across the Tyrrhenian Sea and the Algerian Sea in the western Mediterranean Sea. The MSM72 cruise onboard the German R/V *Maria S. Merian* covered an east-to-west transect across the eastern and western basins as a repeating hydrographic line in GOSHIP (MED1) and a northward transect in the eastern Ionian Sea; in total, 44 stations were sampled. The HaiSec45 cruise on the R/V *Bat-Galim* took place offshore Israel (Haifa) from which we received seawater samples from 8 stations. For all cruises, seawater was collected for nitrate isotopes from surface to bottom using 10 L Niskin bottles attached to a Sea_Bird CTD rosette system (see Hainbucher et al., 2020). Unfiltered seawater was collected in MilliQ-washed HDPE Nalgene bottles which were rinsed generously with sample water before filling. The samples were stored frozen at −20 °C until analysis. Nutrient concentrations (nitrite, nitrate + nitrite, phosphate) were performed onboard with either a four-channel QuAAtro continuous flow analyzer from SEAL analytical (Germany) following the SEAL analytical protocol (MSM72 and TalPro cruises, Hainbucher et al. 2020) or a three-channel segmented flow auto-analyzer system (AA-3, SEAL analytical) (Sisma-Ventura et al., 2022).

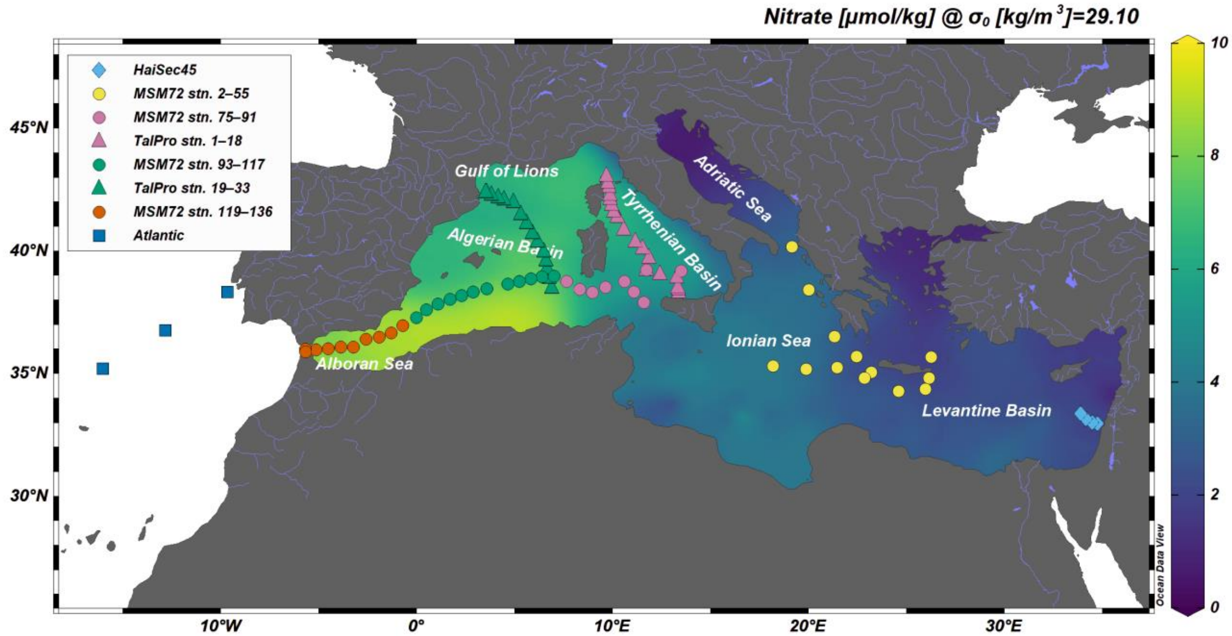

Figure 1. Locations of all water samples plotted over nitrate concentration on the 29.1 kg/m^3 isopycnal, which corresponds to the intermediate water mass. The TalPro cruise stations are indicated with purple (Tyrrhenian section, stations TalPro 1 – 18) and green (Algerian section, stations TalPro 19 – 33) triangles. The MSM72 cruise is shown in colored circles as an east-to-west transect (Zonal transect, eastern stations MSM72 stn. 2 – 13 and MSM72 stn. 47 – 55, western stations MSM72 stn. 75 – 136), and the Ionian section (stations MSM72 stn. 13 – 40) in the eastern basin as a northward transect. The light blue diamonds offshore Israel indicate the HaiSec45 cruise. For reference, the stations outside the Strait of Gibraltar (Atlantic Ocean) are shown as blue squares.

2.2 Nitrate δ^{15}N and δ^{18}O analyses

Samples with nitrate + nitrite concentrations of ≥ 0.3 μmol/kg were analyzed for nitrate δ^{15}N and δ^{18}O in at least duplicates by the ‘denitrifier’ method, in which denitrifying bacteria *Pseudomonas chlororaphis ssp. aureofaciens* (ATCC 13985), lacking an active N_2O reductase, quantitively convert nitrate and nitrite into N_2O (Casciotti et al., 2002; Sigman et al., 2001). The isotopic composition of N_2O was then measured by Gas Chromatography-Isotope Ratio Mass Spectrometry (GC-IRMS) using a Thermo Scientific MAT 253 mass spectrometer coupled to a custom-built N_2O extraction and purification interface (Weigand et al., 2016). Measurements are referenced to air-N_2 for nitrate δ^{15}N and Vienna Standard Mean Ocean Water (VSMOW) for nitrate δ^{18}O using international nitrate reference standards IAEA-NO-3 and USGS34.

Additionally, an in-house standard was run in parallel to assess the long-term reproducibility. The in-house standard consists of seawater nitrate sampled in the deep Atlantic Ocean and diluted with nutrient-depleted seawater to reach the concentration range given by the samples. For a concentration range between 2 μM and 10 μM, the long-term reproducibility (i.e., standard deviation) of the in-house standard for nitrate δ^{15}N and δ^{18}O was 0.1‰ and 0.2‰, respectively. For nitrate + nitrite concentrations of 0.3 – 2 μM higher standard deviations are observed (0.4‰ and 0.6‰ for δ^{15}N and δ^{18}O, respectively). Replicate analyses of the samples between runs indicate a median 1sd reproducibility (i.e., standard deviation) of 0.04‰ and 0.1‰ between 2 μM and 10 μM for δ^{15}N and δ^{18}O, respectively, and 0.1‰ and 0.5‰ for 0.3 – 2 μM, respectively. Errors are given as standard deviation if not otherwise specified.

Even a small proportion of nitrite (NO_2^-) in the nitrate + nitrite pool can affect the isotopic measurement of nitrate δ^{15}N and δ^{18}O significantly (Fawcett et al., 2015; Fripiat et al., 2019; Kemeny et al., 2016). The samples with detectable nitrite concentrations (i.e., with nitrite contribution more than 0.25% of the nitrate + nitrite pool) and samples shallower than 300 m depth were treated with sulfamic acid to remove the nitrite prior to isotopic analysis, yielding nitrate-only isotopic values (Granger & Sigman, 2009). In cases where samples exhibit undetectable nitrite concentrations, isotope measurements represent isotopic values solely associated with nitrate. In this manuscript, we report only nitrate-only δ^{15}N and δ^{18}O values, while the effects of nitrite in the upper ocean and the comparison with nitrate + nitrite data will be interpreted elsewhere.

2.3 Dissolved organic N concentrations and δ^{15}N

Dissolved organic N (DON) measurements are based on the method described by Knapp et al. (2005) where total N (i.e., particulate N, DON, ammonium, nitrite and nitrate) is oxidized to nitrate by mixing 1 mL of persulfate oxidizing reagent (POR) (which is made with 1 g of NaOH dissolved in MilliQ and 1 g of recrystallized $K_2S_2O_8$) with 2 mL of sample. The nitrate is then converted to N_2O using the ‘denitrifier’ method as described above. For the concentration, nitrate is measured by chemiluminescence using a Teledyne NOx analyzer as described in Braman & Hendrix (1989).

To correct for the blank associated with the POR solution, POR blanks were prepared in duplicate along with the samples. Amino acid standards (USGS40 and USGS65) report a long-term reproducibility of 0.2‰, and replicate analyses of the samples indicate a median 1sd reproducibility of 0.2‰. By assuming that there is no significant ammonium and particulate N (PN) accumulation in the samples, DON concentrations are calculated by subtracting the concentrations of nitrate + nitrite from the TN concentrations (e.g., Knapp et al., 2005). DON δ^{15}N is calculated by mass balance, requiring the previously calculated concentrations and the measured δ^{15}N of nitrate + nitrite, and TN:

$$DON\delta^{15}N = (TN\delta^{15}N * [TN] - NO_3^-\delta^{15}N * [NO_3^-])/[DON] \quad (1).$$

Errors on DON concentration and DON δ^{15}N are given as standard deviation if not otherwise specified.

2.4 Box model of the Mediterranean Sea

A prognostic four-box model of the Mediterranean Sea has been developed to better constrain the sources of nitrate into the Mediterranean Sea by using the approach described in Fripiat et al. (2023) for the global ocean. The Mediterranean Sea is divided into four boxes: deep ocean in the western basin, surface waters in the western basin, deep ocean in the eastern basin, surface waters in the eastern basin (Figure 2). The surface water is defined as the upper 100 m of the water column and roughly corresponds to the mixed layer.

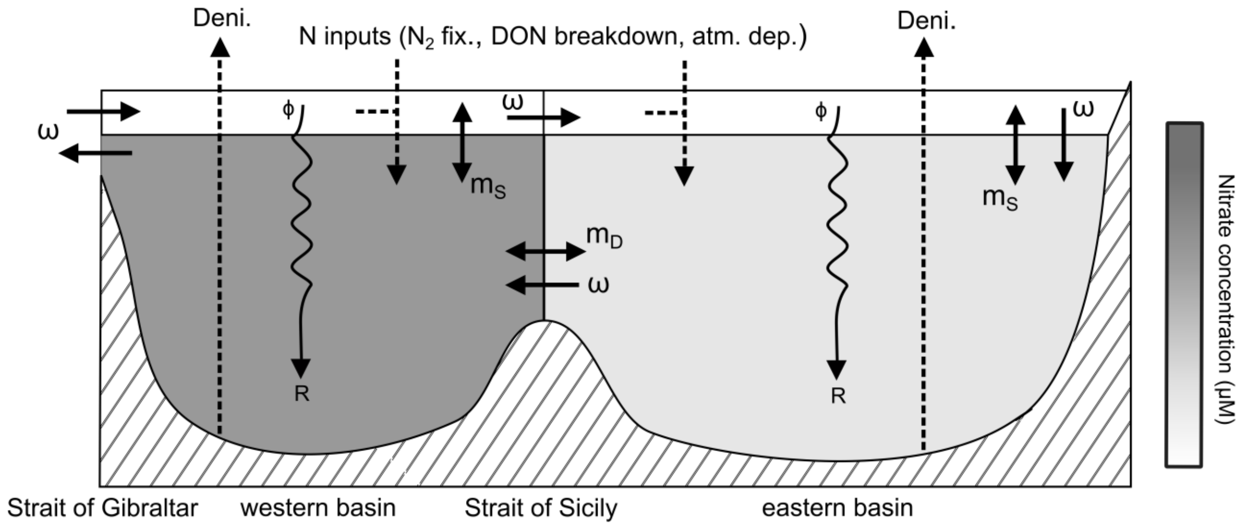

Figure 2. Prognostic four-box model of the Mediterranean Sea. Surface and deep waters of both the western and eastern basin each represent one box, which exchange water and dissolved constituents among each other by advection or mixing. See text for details.

Water and dissolved constituents are exchanged among the different boxes either by advective fluxes (ω) (Bryden et al., 1994; Tsimplis & Bryden, 2000), i.e., anti-estuarine circulation consisting of inflow of Atlantic water through the Strait of Gibraltar at the surface and just below the sill depth which is tidally heaved over the sill into the Mediterranean Sea, and an outflow of dense Mediterranean water, or mixing fluxes (m) between the two deep basin at the Strait of Sicily (m_D) and between surface and deep waters (m_S). The advective flux (ω) transports water from the Atlantic Ocean to the surface waters in the western basin, to the surface waters in the eastern basin, to the deep ocean in the eastern basin, to the deep ocean in the western basin, and to the Atlantic Ocean. The Atlantic Ocean is considered as an infinite and homogeneous reservoir with a range for nitrate and phosphate concentrations of 0.5 – 5.0 μM and 0.03 – 0.35 μM, respectively. These ranges encompass the range given in the literature (Gómez et al., 2000; Powley et al., 2017). The nitrate δ^{15}N of the Atlantic input is set between 4.0‰ and 5.0‰ (Marconi et al., 2015). Export production (∅; i.e., sinking organic matter from the surface to the deep ocean) is controlled by the gross nitrate supply into the surface layers (i.e., water flux times nitrate concentration in the deep ocean) and the degree of nitrate consumption at the surface ($f_{\emptyset}$ = nitrate uptake/gross nitrate supply). We assume full nitrate consumption in surface waters (i.e., $f_{\emptyset}$ = 1). Nitrate assimilation proceeds with a kinetic isotope effect (ε_{ass}) of 5.5‰ (Fripiat et al., 2019), and the δ^{15}N value of export production (∅ δ^{15}N) is described by the Rayleigh fractionation kinetic (accumulated product), making it a function of $f_{\emptyset}$ and ε_{ass}. When nitrate is completely consumed, there is no expression of isotopic discrimination by nitrate assimilation. As a result, the δ^{15}N of export production equals the δ^{15}N of the nitrate supply (Altabet & Francois, 1994). It is assumed that all export production is regenerated (R) in the deep ocean ($N_{Regenerated}$ = N_{Total}-$N_{Preformed}$). The δ^{15}N of the nitrate added to the deep ocean by remineralization is determined by the δ^{15}N of export production (R δ^{15}N = Ø δ^{15}N) (Marconi et al., 2019; Rafter et al., 2013).

An external source of N is supplied to the Mediterranean box (0.0 – 10.0 Tg N yr^{-1}) with a given range for δ^{15}N depending on the tested sources (i.e., N_2 fixation, atmospheric deposition, or partial DON breakdown). We test the model with and without sedimentary denitrification. In the model with sedimentary denitrification (i.e., balancing N_2 fixation), denitrification removes nitrate with an isotope effect of 0‰ (Brandes & Devol, 2002; Lehmann et al., 2007), despite evidence for higher values in specific systems (Alkhatib et al., 2012; Fripiat et al., 2018; Granger et al., 2011; Lehmann et al., 2004, 2007). We do not consider additional sources and sinks of N such as terrestrial river inputs (which appear to have an elevated δ^{15}N; Johannsen et al., 2008; Mayer et al., 2002) or organic matter burial into the sediments.

We run the model in two configurations:

(i) The model is run for 1,000 years, allowing the Mediterranean Sea to reach a steady state. For each model parameter (Table 1), 100,000 random numbers are generated in the parameter sensitivity range, yielding the same number of model scenarios.

(ii) The model is run for 70 years to test the transient anthropogenic perturbation which has increased atmospheric N deposition since 1950 (Preunkert et al., 2003). In addition to model parameters (as described above for (i)), 100,000 random numbers are generated for the initial box conditions, in the range given for the Atlantic Ocean.

Table 1. Model parameters and ranges of the prognostic four-box model.

Model parameters	**Ranges**
ω – anti-estuarine overturning circulation	0.5 – 1.0 Sv
m_D – mixing between the two deep Mediterranean basins	0.0 – 2.0 Sv
m_S – mixing between surface and deep waters in each basin	0.5 – 5.0 Sv
Atlantic nitrate concentration	0.5 – 5.0 μM
Atlantic phosphate concentration	0.03 – 0.35μM
Atlantic nitrate δ^{15}N	4.0 – 5.0‰
Degree of nitrate consumption in the surface waters ($f_{\emptyset}$)	1.0
Remineralization (R)/Export production ($\emptyset$)	1.0
Isotope effect of nitrate assimilation (ε_{ass})	5.5‰
Isotope effect of sedimentary denitrification (ε_{deni})	0.0‰
External N supply of low-δ^{15}N source	0.0 – 10.0 Tg N yr^{-1}
Low-δ^{15}N sources:	
N_2 fixation δ^{15}N	−2.0 – 0.0‰
Atmospheric deposition δ^{15}N	−4.0 – −2.0‰
DON breakdown δ^{15}N	0.0 – 4.0‰

The model best fits are the model scenarios where the model output (nitrate and phosphate concentrations, and nitrate δ^{15}N) falls within the uncertainties given by the weighted observations for the Mediterranean Sea (4.8 – 6.8 μM for nitrate concentration, 0.19 – 0.29 μM for phosphate concentration, and 2.0 – 3.0‰ for nitrate δ^{15}N).

3 Results

3.1 Nitrate concentrations

Low nitrate concentrations prevail in the Mediterranean Sea (~ 5.8 μM for the weighted average) in comparison to the rest of the ocean (~ 30.0 μM), and even more so in the eastern basin (4.6 μM) than in the western basin (8.2 μM) (Figures 3A and 7A). Weighted averages for the Mediterranean Sea are estimated from depth-integrated values from the mean vertical profiles in both the eastern and western basins, and the respective volume for each basin (1.85 x 10^{12} m^3 and 4.01 x 10^{12} m^3, respectively; Sanchez-Cabeza et al., 2002). Nitrate consumption by phytoplankton at the surface yields low nitrate concentrations in all basin surface waters (< 0.1 – 3.6 μM, above MLD), with a nitracline (depth where nitrate concentrations reach or exceed 2 μM) becoming deeper towards the eastern basin (from shallower than 20 m at the Strait of Gibraltar down to ~ 250 m in the eastern basin). Nitrate concentration in intermediate water masses (defined as $O_2 \leq 185\ \mu M$) decreases eastward, from ~ 9.3 μM to ~ 7.0 μM in the easternmost part of the western basin, and ~ 5.5 μM in the eastern basin. Close to the western site of the Sicily strait outlet, in agreement with hydrographic properties (i.e., potential T, salinity), nitrate concentrations show intrusion of nitrate-depleted waters from the eastern basin (Figures 3A and S1). As for intermediate waters, nitrate concentration in deep waters (> 1000 m) decreases eastward, from ~ 8.5 μM down to ~ 5.0 μM in the western and eastern basin, respectively. These patterns are reproduced in the other transects in the Ionian Sea (Figure 4A), the Tyrrhenian basin (Figure 5A), and the Algerian basin (Figure 6A).

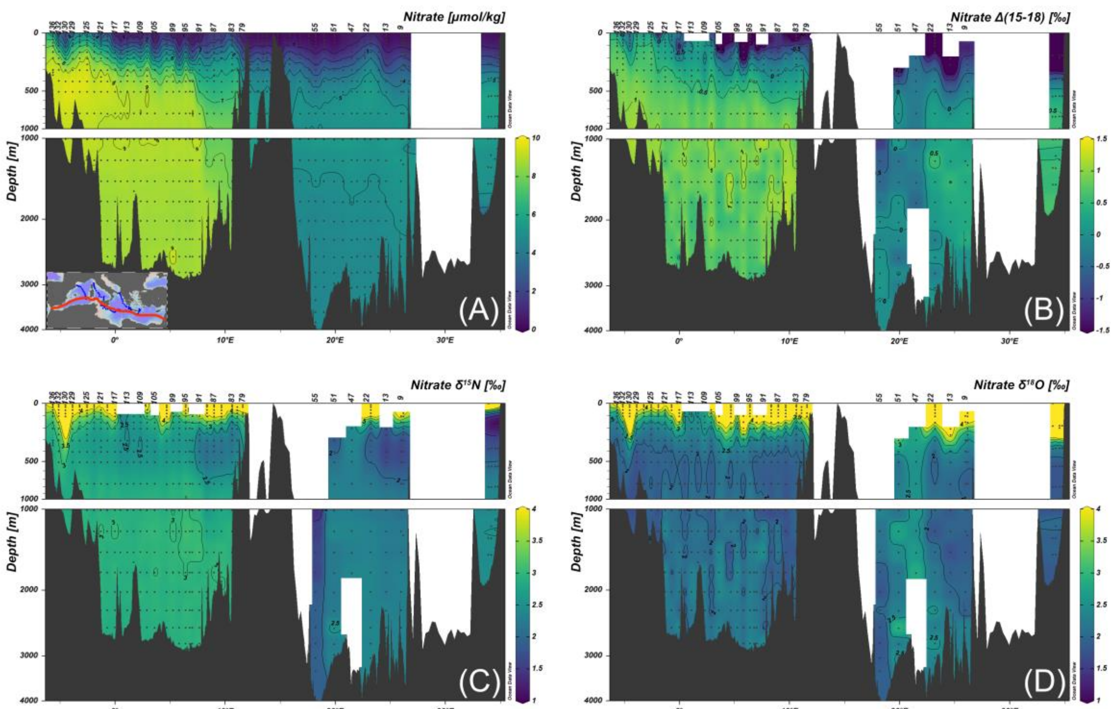

Figure 3. Depth profiles as east-to-west transects across the Mediterranean Sea. (A) nitrate concentration, (B) nitrate Δ(15-18), (C) nitrate δ^{15}N, and (D) nitrate δ^{18}O. Dark gray dots indicate individual samples, while white spaces indicate a lack of data.

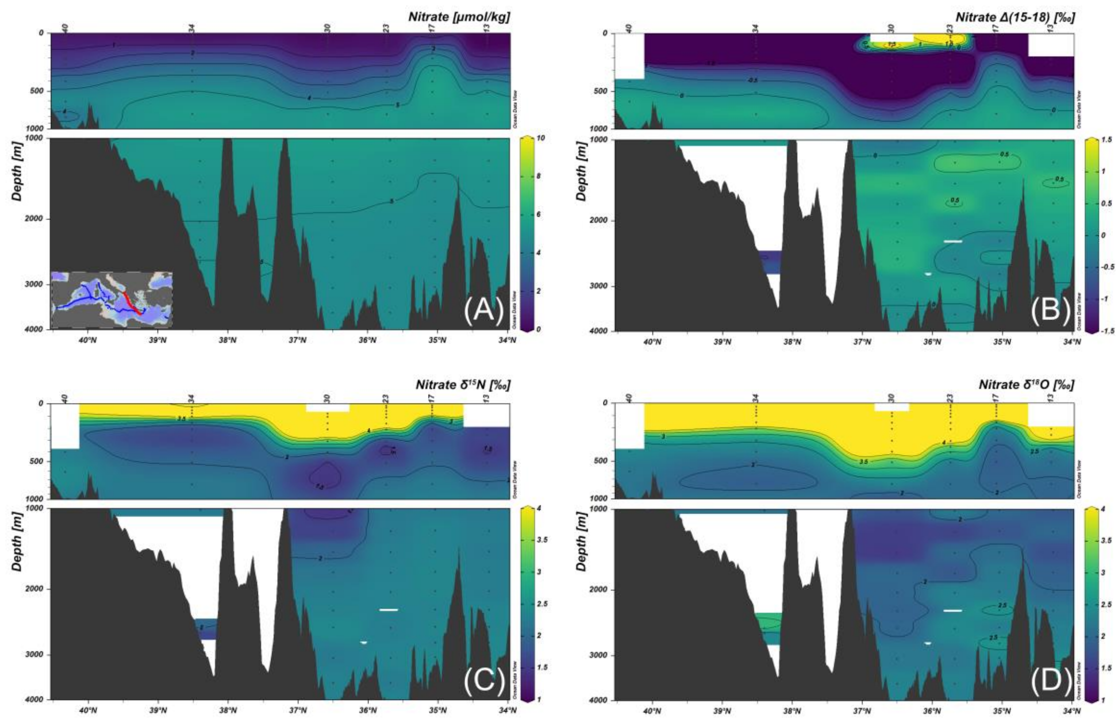

Figure 4. Depth profiles of the Ionian section in the eastern basin of the Mediterranean Sea. (A) nitrate concentration, (B) nitrate Δ(15-18), (C) nitrate δ^{15}N, and (D) nitrate δ^{18}O. Dark gray dots indicate individual samples, while white spaces indicate a lack of data.

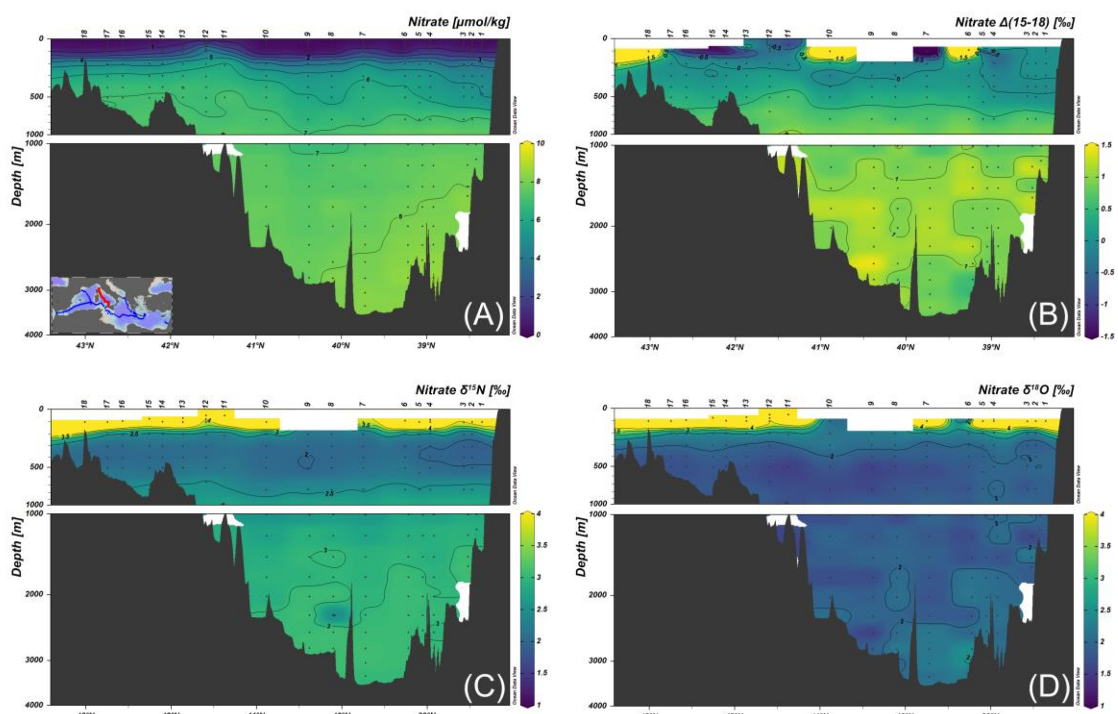

Figure 5. Depth profiles of the Tyrrhenian section in the western Mediterranean Sea. (A) nitrate concentration, (B) nitrate Δ(15-18), (C) nitrate δ^{15}N, and (D) nitrate δ^{18}O. Dark gray dots indicate individual samples, while white spaces indicate a lack of data.

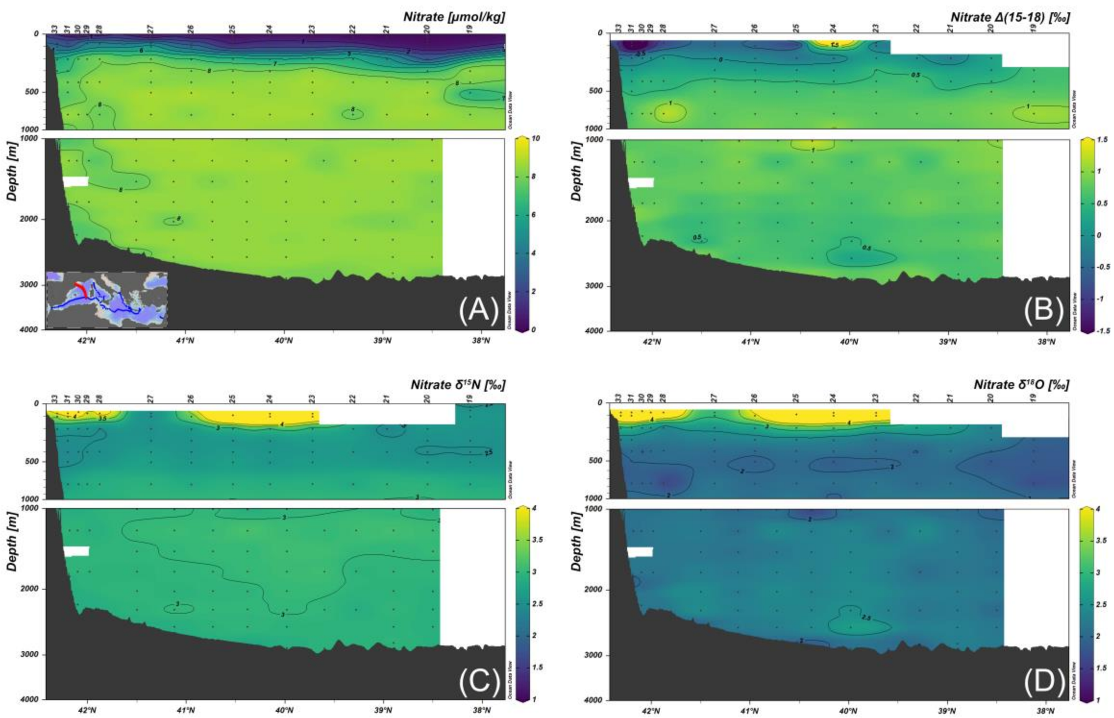

Figure 6. Depth profiles of the Algerian section in the western Mediterranean Sea. (A) nitrate concentration, (B) nitrate Δ(15-18), (C) nitrate δ^{15}N, and (D) nitrate δ^{18}O. Dark gray dots indicate individual samples, while white spaces indicate a lack of data.

3.2 Nitrate δ^{15}N and δ^{18}O

As for the nitrate concentration, the western and eastern Mediterranean Sea differ with respect to nitrate δ^{15}N, but far less for δ^{18}O (Figures 3 and 7). Weighted nitrate δ^{15}N average in the Mediterranean Sea is lower than in the Atlantic Ocean (2.5‰ *vs.* 4.8‰, respectively) (Knapp et al., 2008; Marconi et al., 2015, 2019), with a lower average δ^{15}N value in the eastern basin (2.2‰) than in the western basin (2.9‰). Nitrate δ^{18}O in the Mediterranean Sea is higher than in the Atlantic Ocean (2.2‰ *vs.* 1.8‰, respectively), and relatively constant between the two Mediterranean basins (2.3‰ *vs.* 2.1‰ for the eastern and western basins, respectively). Our measurements agree with previous nitrate δ^{15}N measurements from Pantoja et al. (2002) and Emeis et al. (2010) who reported higher values in the western basin (i.e., 3.4 ± 0.5‰) decreasing eastwards to 2.5 ± 0.1‰, and 2.2 ± 0.3‰ for the eastern basin, respectively. In contrast, we report lower nitrate δ^{18}O values than Emeis et al. (2010) who reported an average nitrate δ^{18}O value of 3.7 ± 0.9‰.

A pronounced elevation in nitrate $\delta^{15}N$ and $\delta^{18}O$ in surface waters is observed across all basins (Figures 3, 4, 5, 6 and 7). In the western basin, nitrate $\delta^{15}N$ and $\delta^{18}O$ values remain relatively constant up to a depth of 200 m, and then increase in parallel up to the surface. The same pattern is observed in the eastern basin, with the exception that nitrate $\delta^{18}O$ values begin to increase at deeper depths in the water column (Figure 7). Phytoplankton preferentially consume ^{14}N- and ^{16}O-bearing nitrate, which leads to an enrichment of residual nitrate pool in ^{15}N and ^{18}O (Fripiat et al., 2019; Granger et al., 2004, 2010; Sigman et al., 1999). In the upper Mediterranean Sea, the negative correlation between nitrate concentration and both nitrate $\delta^{15}N$ and $\delta^{18}O$ is, therefore, a consequence of isotopic fractionation during nitrate assimilation in surface waters (Figures 7A, C and D). The depth structure of nitrate $\delta^{15}N$ and $\delta^{18}O$ in the upper Mediterranean water column will be discussed elsewhere.

In agreement with mean nitrate $\delta^{15}N$ and $\delta^{18}O$ values in the Mediterranean Sea, intermediate water nitrate $\delta^{15}N$ generally increases from east to west (2.1 ± 0.3‰ and 2.6 ± 0.3‰ in the eastern and western basin, respectively), whereas nitrate $\delta^{18}O$ stays almost constant (2.1 ± 0.3‰ and 2.0 ± 0.2‰ in the eastern and western basin, respectively). This pattern is also observed in deep waters for both nitrate $\delta^{15}N$ (2.9 ± 0.1‰ and 2.2 ± 0.2‰ in the western and eastern basin, respectively) and $\delta^{18}O$ (2.1 ± 0.2‰ and 2.2 ± 0.3‰ in the western and eastern basin, respectively). Again, the described isotopic patterns are reproduced by the respective sections in the Ionian Sea, the Tyrrhenian and Algerian basins (Figures 4, 5, 6 and 7).

Nitrate Δ(15-18) values (i.e., nitrate $\delta^{15}N$-nitrate $\delta^{18}O$) are lower in the eastern basin than the western basin, with lower values occurring deeper in the eastern water column. At the scale of the Mediterranean Sea, weighted nitrate Δ(15-18) values (0.3‰ on average) are notably lower than in the North Atlantic (~ 3.1‰; Marconi et al., 2015) (Figures 3, 4, 5, 6 and 7).

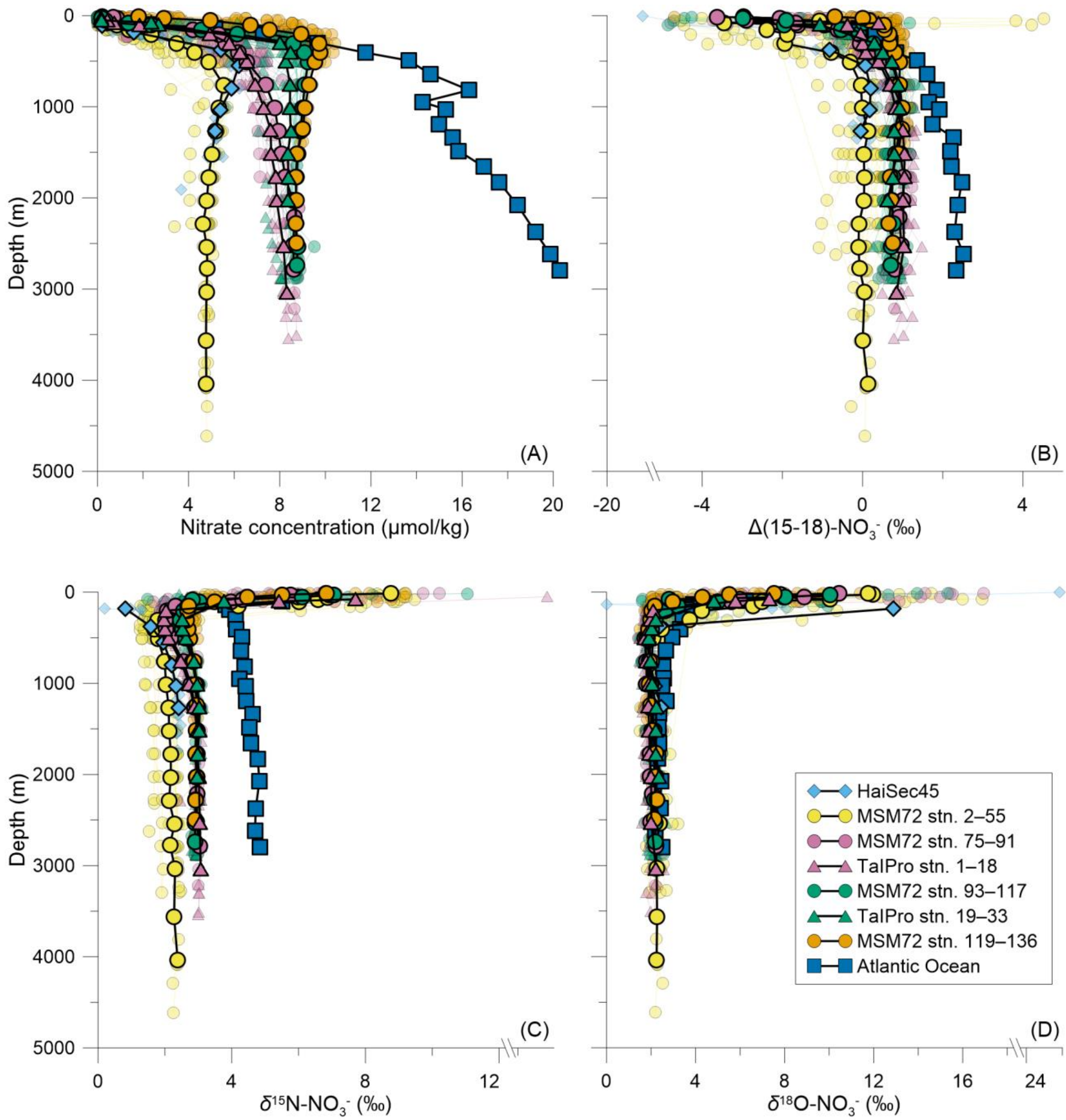

Figure 7. Average depth profiles of nitrate concentration (A), Δ(15-18) (B), nitrate δ^{15}N (C) and nitrate δ^{18}O (D) of the Mediterranean Sea in comparison to the Atlantic Ocean (outside the Strait of Gibraltar, data from Marconi et al., 2015). The nitrate concentration in the Mediterranean Sea is clearly lower relative to the Atlantic Ocean and shows decreasing nitrate concentrations towards the eastern basin, which can also be observed for nitrate δ^{15}N (C). Mediterranean nitrate δ^{18}O is comparable to the Atlantic Ocean with slightly higher average values in the latter (D). Resulting from that, Δ(15-18) yields lower values in the Mediterranean Sea compared to the Atlantic Ocean, with a decreasing trend towards the eastern basin (B). Individual stations are shown as transparent profiles, while thick profiles indicate the means of each basin. For color coding see Figure 1.

3.4 Dissolved organic N concentrations and DON $\delta^{15}N$

DON concentrations are significantly lower than nitrate concentrations and do not exhibit strong differences between the western and eastern basin compared to nitrate concentration (Figures 7A and 8A). Surface waters (0 – 150 m depth) have an average DON concentration of 3.7 ± 0.9 μM, which decreases downward to 2.5 ± 0.6 μM in intermediate waters (defined as $O_2 \leq 185$ μM) and 2.0 ± 0.3 μM in deep waters.

Mediterranean DON $\delta^{15}N$ data generally show higher values than nitrate $\delta^{15}N$ (Figures 7C and 8B). Surface waters indicate lowest DON $\delta^{15}N$ values of 5.3 ± 1.5‰ and 4.3 ± 0.6‰ in the western and eastern basin, respectively, but show an overall enrichment in ^{15}N compared to the Atlantic Ocean (3.9‰) (Knapp et al., 2011) (Figure 8B). Average DON $\delta^{15}N$ increases to intermediate waters to ~ 7.9 ± 1.8‰ in the western and 6.8 ± 1.2‰ in the eastern basin (Figure 8B). In deep waters, DON $\delta^{15}N$ decreases slightly to 7.3 ± 1.4‰ and 6.2 ± 1.4‰ in the western and eastern basin, respectively.

The decrease in average DON concentration of ~ 1.2 μM from surface to intermediate waters is associated with a DON ^{15}N enrichment of ~ 2.5‰, where we observe maximum DON $\delta^{15}N$ values of 9.0 ± 2.5‰ at 1000 m depth (Figure 8B). The estimated isotope effect of DON degradation of 2.8 – 4.8‰ (with one exceptionally high isotope effect of 10.0‰ at the western outlet of the Strait of Sicily) agrees well with other estimates (Figure 8C) (4.9 ± 0.4‰) (Knapp et al., 2018; Zhang et al., 2020), although being in the lower range.

TDN $\delta^{15}N$ measurements have been reported by Emeis et al. (2010) in the eastern basin. Their reported DON $\delta^{15}N$ shows a similar distribution and comparable DON $\delta^{15}N$ values in the eastern basin (~ 6.7 ± 3.5‰ in deep waters).

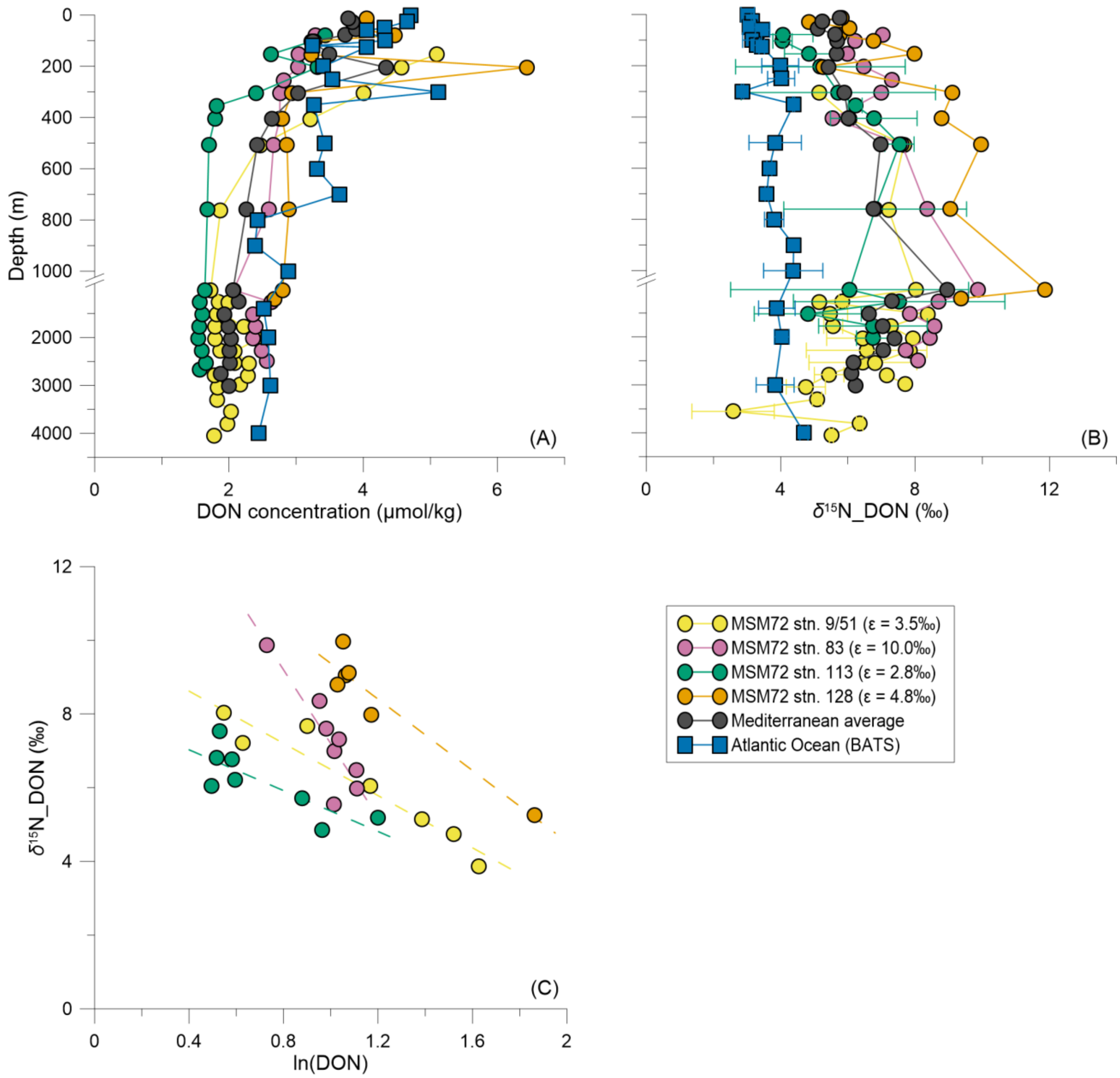

Figure 8. Results of DON measurements as depth profiles. (A) DON concentrations in the Mediterranean Sea (circles) in comparison to the Atlantic Ocean (BATS station, blue squares), (B) DON δ^{15}N of the Mediterranean Sea in comparison to DON δ^{15}N in the Atlantic Ocean (BATS station), (C) DON δ^{15}N *vs.* ln(DON) to estimate the isotope effect of Mediterranean DON degradation based on Rayleigh fractionation kinetics (Mariotti et al., 1981). DON concentrations and isotopes are calculated from TN measurements as described in section 2.4. Error bars in (B) indicate the propagated DON δ^{15}N error. The dark gray symbol set marks the average DON concentration (A) and DON δ^{15}N values (B).

4 Discussion

4.1 Accumulation of low-$\delta^{15}N$ N sources as regenerated nitrate

The observed upward decrease in Δ(15-18), in addition to the weighted low-$\delta^{15}N$ of the Mediterranean Sea, suggests the presence of external low-$\delta^{15}N$ N sources to the Mediterranean Sea. These sources may include N_2 fixation (Carpenter et al., 1997; Minagawa & Wada, 1986; Pantoja et al., 2002), atmospheric deposition of anthropogenic N (Emeis et al., 2010; Mara et al., 2009), and/or the partial breakdown of dissolved organic N (DON) being supplied to the Mediterranean Sea, occurring with an isotopic discrimination (Knapp et al., 2018; Zhang et al., 2020) (see section 4.2). The observation of lower nitrate Δ(15-18) values in the eastern basin and at greater depth relative to the western basin suggests that these additional low-$\delta^{15}N$ N sources of nitrate are supplied to the surface waters and transported with the anti-estuarine circulation.

The east-to-west gradient in nitrate $\delta^{15}N$ and the absence of gradient in nitrate $\delta^{18}O$ implies that the local Mediterranean low-$\delta^{15}N$ nitrate source is mostly passing through the internal N cycling (i.e., nitrate assimilation, export, and remineralization) with the resulting nitrate accumulating at depth as regenerated nutrient. However, we are unable to distinguish whether the low-$\delta^{15}N$ nitrate source initially reaches the interior of the Mediterranean Sea via nitrification or if nitrate with a different origin is subsequently cycled through nitrification within the Mediterranean. Given previously suggested rates of the low-$\delta^{15}N$ N supply terms (less than 4 Tg N yr^{-1}; section 4.2) and internal N cycling (~ 8 Tg N yr^{-1} assuming a C:N ratio of ~ 6 and the estimate of carbon export at 100 m depth by Guyennon et al. (2015)), the latter may be greater.

In the Mediterranean Sea, the nitrate supply from intermediate waters to the surface mixed layer is nearly completely consumed by phytoplankton assimilation in summer (Belgacem et al., 2021; Pujo-Pay et al., 2011). Eventually, this assimilated N is converted to sinking N that leaves the mixed layer before being remineralized in intermediate waters, and flux balance requires that its $\delta^{15}N$ is similar to that of the nitrate supply to the mixed layer (Altabet, 1988). As it passes through the ocean water column, the sinking N is remineralized to ammonium and then nitrified to nitrate. Since nitrification in the ocean interior typically competes with no other processes and is in a steady-state balance with the ammonium production rate, the N isotope fractionation of nitrification has little impact on the $\delta^{15}N$ of nitrate remineralized in the ocean interior. Thus, the $\delta^{15}N$ of the nitrate added to the ocean interior by remineralization is largely determined by the $\delta^{15}N$ of the sinking N from the surface ocean (Marconi et al., 2019; Rafter et al., 2013). Accordingly, the internal cycling of N preserves the east-to-west nitrate $\delta^{15}N$ gradient.

In contrast, the O atoms during nitrification come predominantly from water and the regeneration of nitrate in the ocean interior has a constant $\delta^{18}O$ value, which has been estimated based on field data to be equal to the seawater $\delta^{18}O$ ~ +1‰ (Marconi et al., 2019; Rafter et al., 2013; Sigman et al., 2009). Mediterranean seawater $\delta^{18}O$ measurements show average values of 1.46 ± 0.02‰ (LeGrande & Schmidt, 2006). Based on that, the calculation suggests that the $\delta^{18}O$ value of regenerated nitrate is 0.7 ± 0.4‰ higher than that of seawater (i.e., nitrate-only $\delta^{18}O$-seawater $\delta^{18}O$), which roughly agrees with previous studies (Sigman et al., 2009; Rafter et al., 2013; Marconi et al., 2019). Since the internal N cycle produces relatively constant nitrate $\delta^{18}O$ across the Mediterranean Sea, it preserves the east-to-west gradient in nitrate $\delta^{15}N$ and explains the absence of a gradient for nitrate $\delta^{18}O$.

For the nitrate in the LIW as it flows from the eastern to the western basin through the Strait of Sicily, the fractions of regenerated *vs.* preformed nutrients can be estimated. To do so, we use the Apparent Oxygen Utilization (AOU) and the stoichiometric ratios between oxygen, carbon, and nutrients during organic matter degradation (Pytkowicx, 1971). In the LIW, the maximum in nitrate concentration is accompanied by a minimum in dissolved oxygen levels (≤ 185 μmol/kg) (Figures S1 – S4), pointing to remineralization of sinking organic matter, and shows a good correlation between AOU and nitrate concentration (Figure 9A; R^2= 0.97 and 0.69, and p-value < 0.001 for both the eastern and western basins), further supporting a major contribution of regenerated nitrate to the total nitrate pool. However, the transition from the eastern and Tyrrhenian basin data to the data in the Algerian basin and close to the Strait of Gibraltar indicate that nitrate is added to the western intermediate waters without changing the AOU (Figure 9A, gray arrow). This suggests that ~ 3.0 μM of preformed nitrate is contained in western Mediterranean waters, either from the Atlantic inflow or from deep water formation of partially nitrate-depleted surface waters during winter (Schneider et al., 2014).

Phosphate is used instead of nitrate hereafter to estimate the fraction of regenerated nutrients ($P_{Regenerated}/P_{Total}$) as nitrate could be affected by N_2 fixation and denitrification. Redfield’s stoichiometry leads to unrealistically high regenerated nutrients, resulting in calculations of negative preformed phosphate (Figure S5). Instead, we propose to use the stoichiometric C:P (195:1), N:P (31:1) and C:O (1:150) ratios by Martiny et al. (2013) and Anderson (1995) to estimate the $-O_2$:P ratio for the Mediterranean Sea. For the C:P ratio, we selected the value given by Martiny et al. (2013) in the same latitudinal range (30 – 40° N) as the Mediterranean Sea. The choice of these stoichiometric ratios is further supported by a compilation of organic matter in the Mediterranean Sea (Pujo-Pay et al., 2011). According to the input of preformed nitrate to the western basin via the Atlantic inflow and/or deep water formation, the fraction of regenerated nutrients increases from the western to the eastern Mediterranean Sea (from > 0.5 to 1) (Figures 9B and S6).

The presence of preformed nutrients in the western basin supports that the low-δ^{15}N N sources are progressively mixed with the inflow of high-δ^{15}N preformed nitrate from the Atlantic Ocean towards the west, generating the west-to-east nitrate δ^{15}N gradient. The negative trend of nitrate δ^{15}N with regenerated/total phosphate allows us to calculate the preformed high-δ^{15}N end-member (i.e., 3.8 ± 0.1‰), which is close to the subsurface Atlantic nitrate δ^{15}N (Figures 7C and 9B), in agreement with our hypothesis. The regenerated low-δ^{15}N end-member (i.e., 2.2 ± 0.1‰) represents a mixture between export production fueled by the nitrate supply from intermediate waters to the surface and external local low-δ^{15}N N sources.

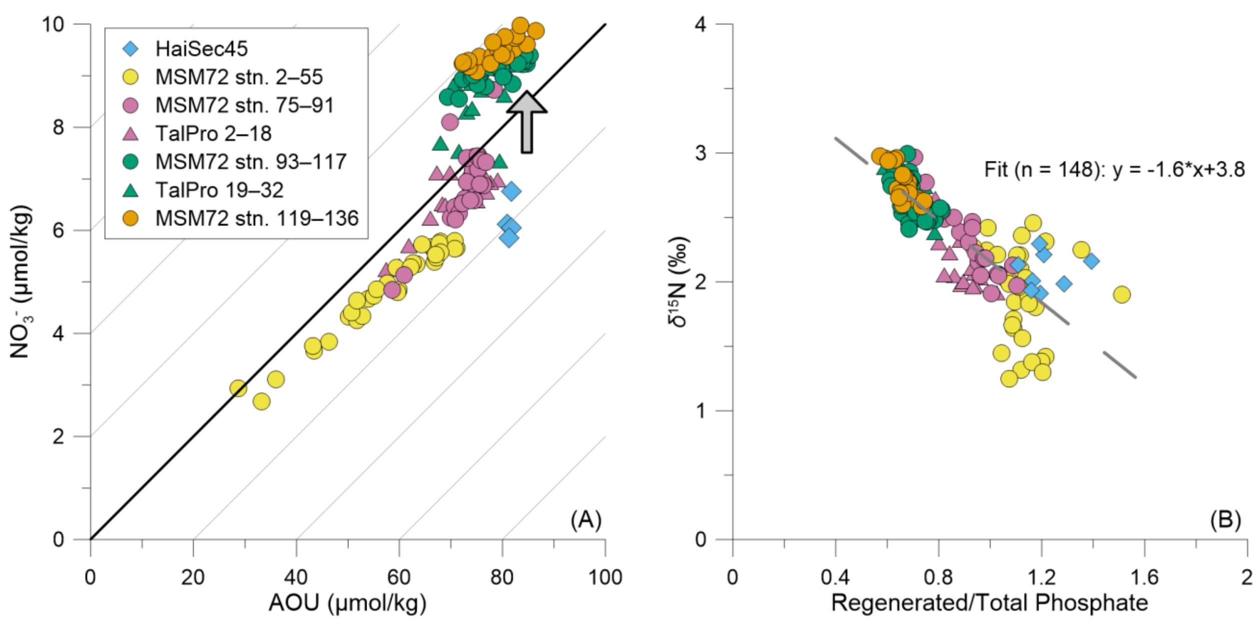

Figure 9. Visualization of the regeneration process in the Mediterranean Sea. (A) shows the positive relationship between AOU and nitrate concentration in intermediate waters, with the nitrate concentration increasing from east to west. The gray arrow indicates the existence of

preformed nitrate in the western basin of ~ 3 μM, introduced from the Atlantic Ocean or from Mediterranean deep water formation. (B) shows the relationship between nitrate δ^{15}N and regenerated/total phosphate, calculated from AOU with the Martiny et al. (2013) stoichiometric ratios.

4.2 Identities and rates of the low-δ^{15}N N sources

Earlier studies suggest that the low-δ^{15}N nitrate in the Mediterranean Sea could be explained by high rates of either N_2 fixation (Pantoja et al., 2002; Sachs & Repeta, 1999) or atmospheric deposition of anthropogenic N (Emeis et al., 2010; Mara et al., 2009). N_2 fixation produces nitrate with a δ^{15}N of 0 – −2‰ (Carpenter et al., 1997; McRose et al., 2019; Minagawa & Wada, 1986) while atmospheric deposition, including both wet and dry, has been reported in the eastern Mediterranean Sea to be at −1 – −5‰ (Mara et al., 2009). These studies used a simple mass and isotopic balance equation to estimate the contribution of these two sources to the Mediterranean nitrate pool, in the form of:

$$\delta^{15}N_{nitrate} = \delta^{15}N_{sinking\ PN} = \frac{\sum \delta^{15}N_{input} * N_{input}}{\sum N_{input}} \quad (2).$$

In the Mediterranean Sea, where nitrate is nearly entirely consumed at the surface, the sinking δ^{15}N of sinking particulate nitrogen (PN) is approximately equal to the δ^{15}N of the nitrate supplied to the surface (Altabet, 1988). These isotopic values can be, therefore, effectively utilized to gauge the proportional contribution of external N inputs into the Mediterranean Sea (Eq. 2). Using this approach, Pantoja et al. (2002) estimated that up to 20% of nitrate in the western basin and up to 90% in the eastern basin may result from N_2 fixation. In contrast, Mara et al. (2009) found out that the nitrogen isotopic composition in the eastern basin can be equally achieved by 50–80% of N deriving from anthropogenic deposition. The similarities in δ^{15}N between the two hypothesized sources make it difficult to distinguish by a simple mass and isotopic balance calculation.

In this study, we revisit the estimates from previous studies by solving the prognostic four-box model equations by varying the model parameters over the ranges presented in Table 1. With this, we target the best agreement between the observations and the model counterpart, in terms of nitrate concentration and nitrate δ^{15}N in the Mediterranean Sea. This approach allows us to account for the coupling between ocean circulation, biogeochemical N dynamics, and different time periods of N supply. In addition to N_2 fixation and atmospheric deposition of anthropogenic N, we also test another source of low-δ^{15}N nitrate to the Mediterranean Sea, i.e., the partial degradation of dissolved organic nitrogen (DON) into nitrate, which occurs with isotopic fractionation (Figure 8c).

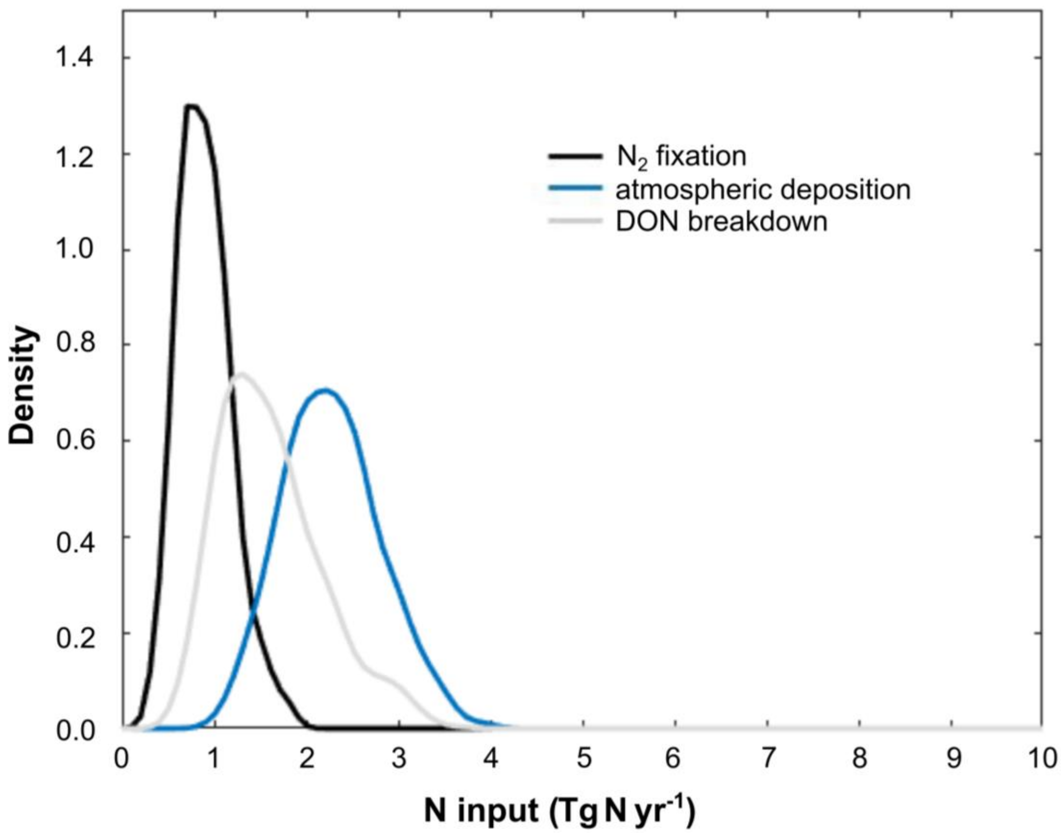

Figure 10. Density function of the model best fits for N_2 fixation, atmospheric deposition of anthropogenic N and partial DON breakdown (in Tg N yr^{-1}).

First, we test if low Mediterranean nitrate δ^{15}N values can be attributed to N_2 fixation. N_2 fixation is prescribed in the model to be occurring entirely in the surface waters and producing new nitrate largely through export production of organic N and its remineralization deeper in the water column. In the model, N_2 fixation introduces new nitrate to the deep box with a δ^{15}N of 0 – −2‰ (Carpenter et al., 1997; McRose et al., 2019; Minagawa & Wada, 1986), and we let the model equilibrate for 1,000 years until reaching a steady state. Accordingly, the model best fits yield a N input of 0.9 ± 0.3 Tg yr^{-1} (0.6 and 1.3 Tg yr^{-1}, 10th and 90th percentile) for N_2 fixation (Figure 10).

Literature estimates for N_2 fixation are reported in μmol m^{-2} d^{-1} (Benavides et al., 2016; Bonnet et al., 2011; Ibello et al., 2010; Rahav et al., 2013; Ridame et al., 2022; Sandroni et al., 2007; Yogev et al., 2011) and must be converted to Tg yr^{-1} to be compared with our model estimates. We assumed that the daily average per unit area (i.e., μmol m^{-2} d^{-1}) is representative of the Mediterranean area (i.e., 2.5 x 10^{12} m^{2}) and over the year. Large differences are reported in some studies for N_2 fixation rates between the western and eastern basin (Bonnet et al., 2011), but not always (Ridame et al., 2022), and no clear seasonal variations have been reported in a timeseries performed in the Ligurian Sea (Sandroni et al., 2007). These literature estimates reported in Tg yr^{-1} are within our model estimates, i.e., 1.2 ± 1.0 Tg yr^{-1} (Sandroni et al., 2007), 0.3 ± 0.2 Tg yr^{-1} (Bonnet et al., 2011), and 1.0 ± 0.3 Tg yr^{-1} (Ridame et al., 2022), suggesting that a modest rate of N_2 fixation alone is sufficient to reproduce the low-δ^{15}N signal in the Mediterranean Sea. The model best fits for nitrate and phosphate concentration in the Atlantic inflow are 3.7 ± 0.5 μM and 0.24 ± 0.03 μM, respectively, for the prognostic four-box model. These estimated values are close to the nitrate and phosphate concentrations measured at the Strait of Gibraltar (Huertas et al., 2012).

A positive relationship is reported between nitrate supply from the Atlantic Ocean and the rates of N_2 fixation necessary to reproduce the weighted nitrate δ^{15}N value of the Mediterranean Sea (Figures 11A, B). If there is a larger nitrate supply from the Atlantic Ocean, a larger rate of N_2 fixation is required to explain the decrease in nitrate δ^{15}N in the Mediterranean Sea. Huertas et al. (2012) estimate the nitrate supply at the Strait of Gibraltar at 2 Tg N yr^{-1}, close to the model best fits (1.4 ± 0.3 Tg N yr^{-1}).

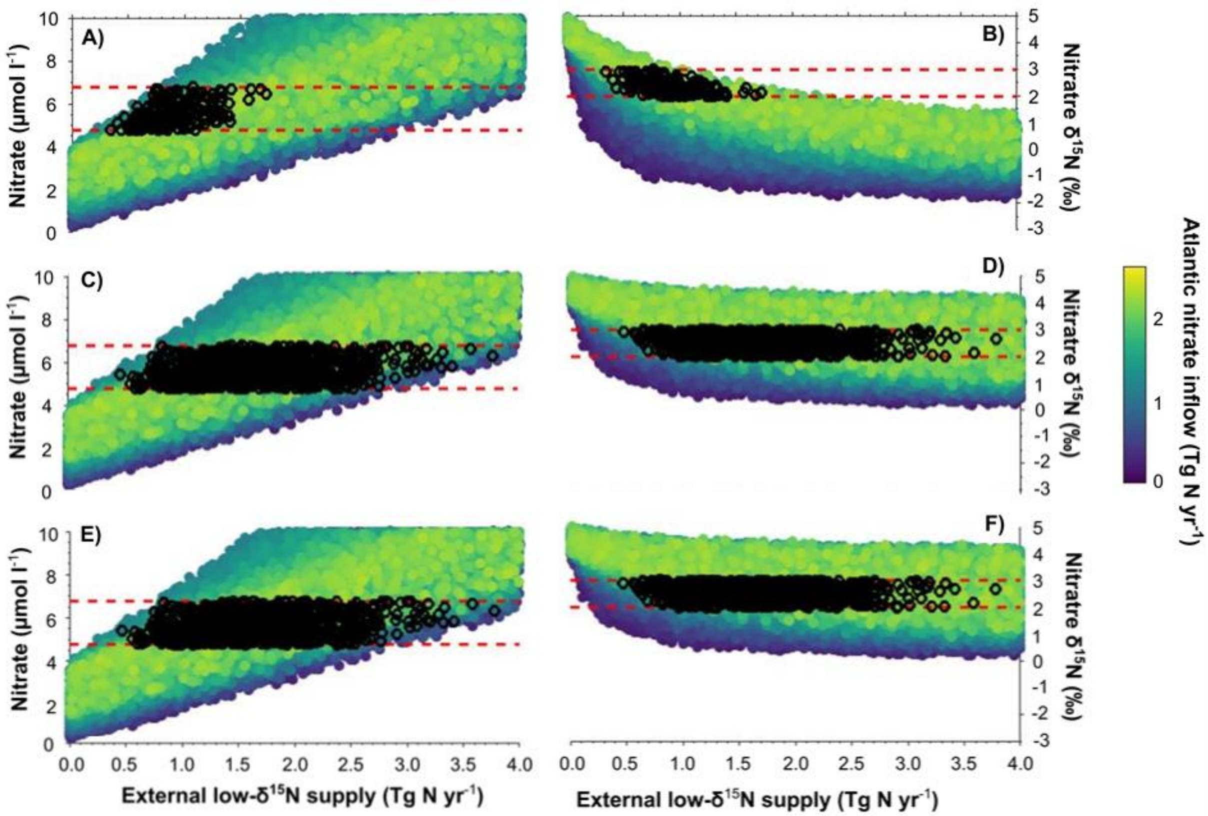

Figure 11. Model estimates of nitrate concentration (A, C, E) and nitrate δ^{15}N (B, D, F) *vs.* the rate of external low-δ^{15}N N supply (x-axis; in Tg N yr^{-1}) and as a function of nitrate supply from the Atlantic Ocean (color scale in Tg N yr^{-1}). Panels (A, B) are for N_2 fixation, panels (C, D) for atmospheric deposition of anthropogenic N, and panels (E, F) for partial DON breakdown. Black empty circles represent model best fits within the range of Mediterranean weighted averages (red dashed lines).

An interesting aspect of the prognostic four-box model is that the east-to-west gradient in nitrate δ^{15}N is spontaneously reproduced in the model, and the strength of this gradient is mostly a function of the ratio between advective (ω) and mixing flux (m_D) and the ratio between N_2 fixation rates and the Atlantic nitrate supply at the Strait of Gibraltar (Figure 12). A large mixing flux homogenizes the Mediterranean Sea with no more difference between the western and eastern basins. Lower N_2 fixation rates compared to the Atlantic nitrate supply maintains the east-to-west gradient in nitrate δ^{15}N. However, too low N_2 fixation rates imply minimal supply of low-δ^{15}N nitrate and, therefore, no east-to-west gradient in nitrate δ^{15}N.

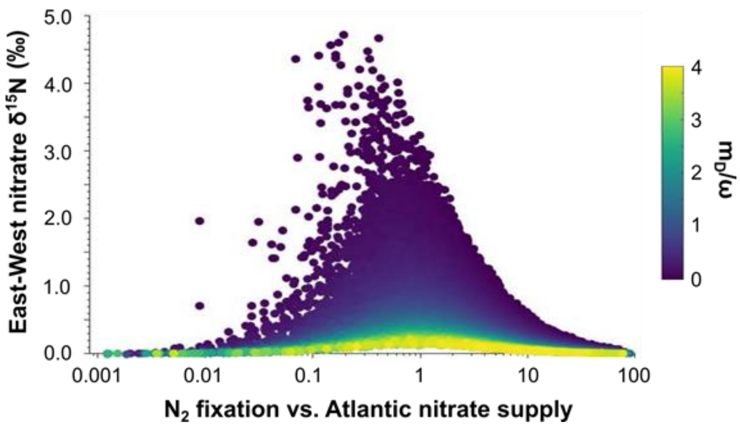

Figure 12. Dependence of the east-to-west nitrate δ^{15}N gradient on the ratio between N_2 fixation and the Atlantic nitrate inflow (x-axis) and the ratio between advective (ω) and mixing flux (m_D) (color scale).

In the model configuration with sedimentary denitrification balancing N_2 fixation, we are unable to reproduce the weighted nitrate concentration of the Mediterranean Sea (Figure S7C). In this case, nitrate concentration stays at the Atlantic inflow concentration, inconsistent with observations. Nevertheless, the nitrate δ^{15}N remains unchanged regardless of whether sedimentary denitrification is considered in our model or not, as we impose no isotopic discrimination for sedimentary denitrification in the model, consistent with the literature (Brandes & Devol, 2002; Lehmann et al., 2004; c.f. Fripiat et al., 2018; Granger et al., 2011). Given the presence of sedimentary denitrification in the Mediterranean Sea (e.g., Powley et al., 2017), the external N supply must exceed this removal term in order to reproduce the observed accumulation of nitrate relative to the Atlantic nitrate inflow.

The second hypothesis is related to atmospheric deposition of anthropogenic N (Emeis et al., 2010), with a weighted annual δ^{15}N of atmospheric deposition of −3.1‰ (Mara et al., 2009). The latter study reports a range for wet and dry nitrate deposition from −1‰ to −5‰. To test this hypothesis, the prognostic four-box model is run for a transient time of 70 years, since anthropogenic input to the Mediterranean Sea has significantly increased since then (Preunkert et al., 2003). Model best fits show that 2.3 ± 0.5 Tg yr^{-1} (1.7 and 2.9 Tg yr^{-1}, 10th and 90th percentile) has to be provided by atmospheric deposition to produce the observed Mediterranean patterns (Figures 10 and 11C, D). The simulated values of atmospheric deposition of anthropogenic N are in the range of values given in a compilation of atmospheric nitrate, ammonium, and DON deposition in the Mediterranean Sea of 1.8 Tg yr^{-1} and 3.3 Tg yr^{-1} if we consider nitrate and ammonium, or nitrate, ammonium, and DON individually (Powley et al., 2014). Once again, the model best fits yield nitrate and phosphate concentrations in the Atlantic inflow that are consistent with the literature (Huertas et al., 2012), of 4.4 ± 0.4 μM and 0.25 ± 0.03 μM, respectively. This analysis suggests that, as for N_2 fixation, atmospheric N deposition alone is sufficient to reproduce the low nitrate δ^{15}N signal in the Mediterranean Sea.

An alternative and/or additional explanation for the low δ^{15}N values in the Mediterranean Sea is the partial degradation of dissolved organic N (DON) supplied by the Atlantic. This process has been reported with an associated isotopic effect of ~ 4.9 ± 0.4‰ (e.g., Hannides et al., 2013; Knapp et al., 2018; Zhang et al., 2020), consistent with our data from the Mediterranean (Figure 8). Net degradation of Atlantic DON within the Mediterranean Sea is supported by lower DON concentrations and higher DON δ^{15}N values in the Mediterranean relative to the Atlantic (Figures 8A, B). To estimate the nitrate δ^{15}N of the degradation process (i.e., $\delta^{15}N_{DONdeg}$), we perform a mass and isotopic balance calculation by assuming that the DON pool at 150 m depth (i.e., DON_{150}) is degraded down to a DON concentration at 1000 m depth (i.e., DON_{1000}), as follows:

$$[DON_{150}] * \delta^{15}N_{DON150} = [DON_{1000}] * \delta^{15}N_{DON1000} + \left[DON_{deg}\right] * \delta^{15}N_{DONdeg} \qquad (3).$$

Solving equation (3) for $\delta^{15}N_{DONdeg}$ gives a δ^{15}N value of 2.5 ± 3.2‰ (propagated error based on 1sd; depth ranges: 100 – 300 m and 750 – 1250 m). Our mass balance calculated value encompasses the range given by the accumulated product from the Rayleigh fractionation kinetics, i.e., ~ 0.0 – 1.7‰. We assume for the latter an initial DON δ^{15}N of 4.3 – 5.3‰ (i.e., surface values of the eastern and western basins), a degree of DON consumption of 0.35 – 0.44 (i.e., = 1-$[DON]_{1000}/[DON]_{150}$) and an isotope effect of 4.9 ± 0.4‰. Accordingly, in the prognostic four-box model, the partial DON degradation is prescribed to be at 0.0‰ and 4.0‰, and we let the model equilibrate for 1,000 years until reaching a steady state. The model best fits yield a N input of 1.7 ± 0.6 Tg yr^{-1} (1.0 and 2.5 Tg yr^{-1}, 10th and 90th percentile) for partial DON breakdown, when occurring in isolation (Figures 10 and 11E, F).

If we consider the difference between average DON concentration from our measurements of 3.7 μM in surface waters and 2.0 μM in deep waters as indicative of the DON degradation in the Mediterranean Sea, it suggests that 139 Tg of DON has undergone degradation. Dividing this quantity by the estimated water residence time in the Mediterranean

Sea (120 – 170 years, i.e., $\omega/V_{Mediterranean\ Sea}$), it yields a DON breakdown rate of 1.0 ± 0.2 Tg yr^{-1}, which is slightly lower than the model best fits (i.e., 1.6 ± 0.6 Tg y^{-1}). Consequently, the degradation of DON might account for a significant proportion, but not all, of the observed nitrate δ^{15}N lowering in the Mediterranean. The tendency for this mechanism to yield lower nutrient concentrations for the Atlantic inflow (2.2 ± 0.6 μM *vs.* 3.1 ± 0.3 μM; Huertas et al., 2012) is consistent with this mechanism providing at best a partial explanation of Mediterranean nitrate δ^{15}N lowering.

Based on these results, it is difficult to distinguish between N_2 fixation, atmospheric deposition, and partial DON degradation in driving the low nitrate δ^{15}N observed in the Mediterranean Sea. To further address this question, one possibility would be to reconstruct past nitrate δ^{15}N values in the Mediterranean Sea using fossil-bound δ^{15}N analyses. Fossil-bound δ^{15}N, such as in foraminifera or corals, approximates nitrate δ^{15}N of the shallow thermocline in nutrient-depleted areas (Ren et al., 2009; Smart et al., 2018; Wang et al., 2014), and it preserves this signal in the geological record (Martínez-García et al., 2022). If the anthropogenic input is responsible for the low nitrate δ^{15}N in the Mediterranean Sea, higher fossil-bound δ^{15}N values (i.e., close to the Atlantic inflow nitrate δ^{15}N) should be, therefore, expected in fossil samples from prior to the 1950s.

5 Conclusions

In summary, our study provides a comprehensive overview of the distribution of nitrate δ^{15}N and δ^{18}O throughout the entire Mediterranean Sea. Our findings confirm previous studies, indicating a basin-wide ^{15}N depletion in the Mediterranean Sea compared to the global ocean. This implies the existence of an external, low-δ^{15}N N source contributing to the Mediterranean Sea, in agreement with studies by Pantoja et al. (2002), Mara et al. (2009) and Emeis et al. (2010). Our analysis reveals that the inflow of Atlantic waters through the Strait of Gibraltar dilutes this external, low-δ^{15}N N supply and generates the observed east-to-west gradient in nitrate δ^{15}N in the Mediterranean Sea. Moreover, this external nitrogen supply predominantly accumulates as regenerated nitrate in the interior waters of the Mediterranean.

We present a prognostic four-box model of the Mediterranean Sea, illustrating that modest contributions from N_2 fixation and anthropogenic nitrogen deposition, either individually or combined, can account for the observed low-δ^{15}N signature. Furthermore, we report evidence that partial degradation (with isotopic fractionation) of dissolved organic nitrogen, introduced into the Mediterranean Sea from the Atlantic Ocean, may represent an additional source of low-δ^{15}N nitrate. The capacity for multiple mechanism to explain the low δ^{15}N of nitrate in the Mediterranean Sea is a consequence of the relatively long residence time of water in the basin relative to the inflow at the Strait of Gibraltar.

Acknowledgments

This study was funded by the Max Planck Society. We gratefully acknowledge the support by the scientists and crew from the MSM72, TalPro2016 and HaiSec45 cruises for sampling Mediterranean waters, and Maayan Yehudai for transporting the HaiSec45 samples from Israel to Germany. Furthermore, we would like to thank the S/Y Eugen Seibold crew with the Siemens Foundation for collecting seawater which has been used for the in-house standard preparation at MPIC. A special thanks goes to Barbara Hinnenberg, Mareike Schmitt and Florian Rubach for their lab support. Y.R. and D.M.S. were supported by US NSF grants 1736652 and 1851430 (to D.M.S.). F.F. thanks the FNRS-FRS and the FWB for their financial support in the frame of the EQP U.N029.23 ENGAGE project and the ARC consolidation project STEREO.

Open Research

Data Availability Statement

Data of this study will be uploaded into the PANGAEA database once the paper has been accepted. The model described in this article will be uploaded to a Github repository once the paper has been accepted.

References

Alkhatib, M., Lehmann, M. F., & del Giorgio, P. A. (2012). The nitrogen isotope effect of benthic remineralization-nitrification-denitrification coupling in an estuarine environment. *Biogeosciences*, *9*(5), 1633–1646. https://doi.org/10.5194/bg-9-1633-2012

Altabet, M. A. (1988). Variations in nitrogen isotopic composition between sinking and suspended particles: Implications for nitrogen cycling and particle transformation in the open ocean. *Deep Sea Research Part A. Oceanographic Research Papers*, *35*(4), 535–554. https://doi.org/10.1016/0198-0149(88)90130-6

Altabet, M. A., & Francois, R. (1994). Sedimentary nitrogen isotopic ratio as a recorder for surface ocean nitrate utilization. *Global Biogeochemical Cycles*, *8*(1), 103–116. https://doi.org/10.1029/93GB03396

Anderson, L. A. (1995). On the hydrogen and oxygen content of marine phytoplankton. *Deep Sea Research Part I: Oceanographic Research Papers*, *42*(9), 1675–1680. https://doi.org/10.1016/0967-0637(95)00072-E

Belgacem, M., Schroeder, K., Barth, A., Troupin, C., Pavoni, B., Raimbault, P., Garcia, N., Borghini, M., & Chiggiato, J. (2021). Climatological distribution of dissolved inorganic nutrients in the western Mediterranean Sea (1981–2017). *Earth System Science Data*, *13*(12), 5915–5949. https://doi.org/10.5194/essd-13-5915-2021

Benavides, M., Bonnet, S., Hernández, N., Martínez-Pérez, A. M., Nieto-Cid, M., Álvarez-Salgado, X. A., Baños, I., Montero, M. F., Mazuecos, I. P., Gasol, J. M., Osterholz, H., Dittmar, T., Berman-Frank, I., & Arístegui, J. (2016). Basin-wide N2 fixation in the deep waters of the Mediterranean Sea. *Global Biogeochemical Cycles*, *30*(6), 952–961. https://doi.org/10.1002/2015GB005326

Bethoux, J. P. (1989). Oxygen consumption, new production, vertical advection and environmental evolution in the Mediterranean Sea. *Deep Sea Research Part A. Oceanographic Research Papers*, *36*(5), 769–781. https://doi.org/10.1016/0198-0149(89)90150-7

Béthoux, J. P., Morin, P., Chaumery, C., Connan, O., Gentili, B., & Ruiz-Pino, D. (1998). Nutrients in the Mediterranean Sea, mass balance and statistical analysis of concentrations with respect to environmental change. *Marine Chemistry*, *63*(1), 155–169. https://doi.org/10.1016/S0304-4203(98)00059-0

Bonnet, S., Grosso, O., & Moutin, T. (2011). Planktonic dinitrogen fixation along a longitudinal gradient across the Mediterranean Sea during the stratified period (BOUM cruise). *Biogeosciences*, *8*(8), 2257–2267. https://doi.org/10.5194/bg-8-2257-2011

Braman, R. S., & Hendrix, S. A. (1989). Nanogram nitrite and nitrate determination in environmental and biological materials by vanadium (III) reduction with chemiluminescence detection. *Analytical Chemistry*, *61*(24), 2715–2718. https://doi.org/10.1021/ac00199a007

Brandes, J. A., & Devol, A. H. (2002). A global marine-fixed nitrogen isotopic budget: Implications for Holocene nitrogen cycling. *Global Biogeochemical Cycles*, *16*(4), 67-1-67–14. https://doi.org/10.1029/2001GB001856

Bryden, H. L., Candela, J., & Kinder, T. H. (1994). Exchange through the Strait of Gibraltar. *Progress in Oceanography*, *33*(3), 201–248. https://doi.org/10.1016/0079-6611(94)90028-0

Carpenter, E. J., Harvey, H. R., Fry, B., & Capone, D. G. (1997). Biogeochemical tracers of the marine cyanobacterium Trichodesmium. *Deep Sea Research Part I: Oceanographic Research Papers*, *44*(1), 27–38. https://doi.org/10.1016/S0967-0637(96)00091-X

Casciotti, K. L., Sigman, D. M., Hastings, M. G., Böhlke, J. K., & Hilkert, A. (2002). Measurement of the Oxygen Isotopic Composition of Nitrate in Seawater and Freshwater Using the Denitrifier Method. *Analytical Chemistry*, *74*(19), 4905–4912. https://doi.org/10.1021/ac020113w

Emeis, K.-C., Mara, P., Schlarbaum, T., Möbius, J., Dähnke, K., Struck, U., Mihalopoulos, N., & Krom, M. (2010). External N inputs and internal N cycling traced by isotope ratios of nitrate, dissolved reduced nitrogen, and particulate nitrogen in the eastern Mediterranean Sea. *Journal of Geophysical Research: Biogeosciences*, *115*(G4). https://doi.org/10.1029/2009JG001214

Fawcett, S. E., Ward, B. B., Lomas, M. W., & Sigman, D. M. (2015). Vertical decoupling of nitrate assimilation and nitrification in the Sargasso Sea. *Deep Sea Research Part I: Oceanographic Research Papers*, *103*, 64–72. https://doi.org/10.1016/j.dsr.2015.05.004

Fripiat, F., Declercq, M., Sapart, C. J., Anderson, L. G., Bruechert, V., Deman, F., Fonseca-Batista, D., Humborg, C., Roukaerts, A., Semiletov, I. P., & Dehairs, F. (2018). Influence of the bordering shelves on nutrient distribution in the Arctic halocline inferred from water column nitrate isotopes. *Limnology and Oceanography*, *63*(5), 2154–2170. https://doi.org/10.1002/lno.10930

Fripiat, F., Martínez-García, A., Fawcett, S. E., Kemeny, P. C., Studer, A. S., Smart, S. M., Rubach, F., Oleynik, S., Sigman, D. M., & Haug, G. H. (2019). The isotope effect of nitrate assimilation in the Antarctic Zone: Improved estimates and paleoceanographic implications. *Geochimica et Cosmochimica Acta*, *247*, 261–279. https://doi.org/10.1016/j.gca.2018.12.003

Fripiat, F., Sigman, D. M., Martínez-García, A., Marconi, D., Ai, X. E., Auderset, A., Fawcett, S. E., Moretti, S., Studer, A. S., & Haug, G. H. (2023). The Impact of Incomplete Nutrient Consumption in the Southern

Ocean on Global Mean Ocean Nitrate δ15N. *Global Biogeochemical Cycles*, *37*(2), e2022GB007442. https://doi.org/10.1029/2022GB007442

Gómez, F., González, N., Echevarría, F., & García, C. M. (2000). Distribution and Fluxes of Dissolved Nutrients in the Strait of Gibraltar and its Relationships to Microphytoplankton Biomass. *Estuarine, Coastal and Shelf Science*, *51*(4), 439–449. https://doi.org/10.1006/ecss.2000.0689

Granger, J., Prokopenko, M. G., Sigman, D. M., Mordy, C. W., Morse, Z. M., Morales, L. V., Sambrotto, R. N., & Plessen, B. (2011). Coupled nitrification-denitrification in sediment of the eastern Bering Sea shelf leads to 15N enrichment of fixed N in shelf waters. *Journal of Geophysical Research: Oceans*, *116*(C11). https://doi.org/10.1029/2010JC006751

Granger, J., & Sigman, D. M. (2009). Removal of nitrite with sulfamic acid for nitrate N and O isotope analysis with the denitrifier method. *Rapid Communications in Mass Spectrometry*, *23*(23), 3753–3762. https://doi.org/10.1002/rcm.4307

Granger, J., Sigman, D. M., Needoba, J. A., & Harrison, P. J. (2004). Coupled nitrogen and oxygen isotope fractionation of nitrate during assimilation by cultures of marine phytoplankton. *Limnology and Oceanography*, *49*(5), 1763–1773. https://doi.org/10.4319/lo.2004.49.5.1763

Granger, J., Sigman, D. M., Rohde, M. M., Maldonado, M. T., & Tortell, P. D. (2010). N and O isotope effects during nitrate assimilation by unicellular prokaryotic and eukaryotic plankton cultures. *Geochimica et Cosmochimica Acta*, *74*(3), 1030–1040. https://doi.org/10.1016/j.gca.2009.10.044

Guyennon, A., Baklouti, M., Diaz, F., Palmieri, J., Beuvier, J., Lebaupin-Brossier, C., Arsouze, T., Béranger, K., Dutay, J.-C., & Moutin, T. (2015). New insights into the organic carbon export in the Mediterranean Sea from 3-D modeling. *Biogeosciences*, *12*(23), 7025–7046. https://doi.org/10.5194/bg-12-7025-2015

Hainbucher, D., Álvarez, M., Astray Uceda, B., Bachi, G., Cardin, V., Celentano, P., Chaikalis, S., del Mar Chaves Montero, M., Civitarese, G., Fajar, N. M., Fripiat, F., Gerke, L., Gogou, A., Guallart, E. F., Gülk, B., El Rahman Hassoun, A., Lange, N., Rochner, A., Santinelli, C., … Welsch, A. (2020). Physical and biogeochemical parameters of the Mediterranean Sea during a cruise with RV *Maria S. Merian* in March 2018. *Earth System Science Data*, *12*(4), 2747–2763. https://doi.org/10.5194/essd-12-2747-2020

Hannides, C. C. S., Popp, B. N., Choy, C. A., & Drazen, J. C. (2013). Midwater zooplankton and suspended particle dynamics in the North Pacific Subtropical Gyre: A stable isotope perspective. *Limnology and Oceanography*, *58*(6), 1931–1946. https://doi.org/10.4319/lo.2013.58.6.1931

Huertas, I. E., Ríos, A. F., García-Lafuente, J., Navarro, G., Makaoui, A., Sánchez-Román, A., Rodriguez-Galvez, S., Orbi, A., Ruíz, J., & Pérez, F. F. (2012). Atlantic forcing of the Mediterranean oligotrophy. *Global Biogeochemical Cycles*, *26*(2). https://doi.org/10.1029/2011GB004167

Ibello, V., Cantoni, C., Cozzi, S., & Civitarese, G. (2010). First basin-wide experimental results on N2 fixation in the open Mediterranean Sea. *Geophysical Research Letters*, *37*(3). https://doi.org/10.1029/2009GL041635

Johannsen, A., Dähnke, K., & Emeis, K. (2008). Isotopic composition of nitrate in five German rivers discharging into the North Sea. *Organic Geochemistry*, *39*(12), 1678–1689. https://doi.org/10.1016/j.orggeochem.2008.03.004

Kemeny, P. C., Weigand, M. A., Zhang, R., Carter, B. R., Karsh, K. L., Fawcett, S. E., & Sigman, D. M. (2016). Enzyme-level interconversion of nitrate and nitrite in the fall mixed layer of the Antarctic Ocean. *Global Biogeochemical Cycles*, *30*(7), 1069–1085. https://doi.org/10.1002/2015GB005350

Knapp, A. N., Casciotti, K. L., & Prokopenko, M. G. (2018). Dissolved Organic Nitrogen Production and Consumption in Eastern Tropical South Pacific Surface Waters. *Global Biogeochemical Cycles*, *32*(5), 769–783. https://doi.org/10.1029/2017GB005875

Knapp, A. N., DiFiore, P. J., Deutsch, C., Sigman, D. M., & Lipschultz, F. (2008). Nitrate isotopic composition between Bermuda and Puerto Rico: Implications for N2 fixation in the Atlantic Ocean. *Global Biogeochemical Cycles*, *22*(3). https://doi.org/10.1029/2007GB003107

Knapp, A. N., Sigman, D. M., & Lipschultz, F. (2005). N isotopic composition of dissolved organic nitrogen and nitrate at the Bermuda Atlantic Time-series Study site. *Global Biogeochemical Cycles*, *19*(1). https://doi.org/10.1029/2004GB002320

Knapp, A. N., Sigman, D. M., Lipschultz, F., Kustka, A. B., & Capone, D. G. (2011). Interbasin isotopic correspondence between upper-ocean bulk DON and subsurface nitrate and its implications for marine nitrogen cycling. *Global Biogeochemical Cycles*, *25*(4). https://doi.org/10.1029/2010GB003878

Kress, N., & Herut, B. (2001). Spatial and seasonal evolution of dissolved oxygen and nutrients in the Southern Levantine Basin (Eastern Mediterranean Sea): Chemical characterization of the water masses and inferences on the N:P ratios. *Deep Sea Research Part I: Oceanographic Research Papers*, *48*(11), 2347–2372. https://doi.org/10.1016/S0967-0637(01)00022-X

Krom, M. D., Emeis, K.-C., & Van Cappellen, P. (2010). Why is the Eastern Mediterranean phosphorus limited? *Progress in Oceanography*, *85*(3), 236–244. https://doi.org/10.1016/j.pocean.2010.03.003

Krom, M. D., Herut, B., & Mantoura, R. F. C. (2004). Nutrient budget for the Eastern Mediterranean: Implications for phosphorus limitation. *Limnology and Oceanography*, *49*(5), 1582–1592. https://doi.org/10.4319/lo.2004.49.5.1582

Krom, M. D., Kress, N., Brenner, S., & Gordon, L. I. (1991). Phosphorus limitation of primary productivity in the eastern Mediterranean Sea. *Limnology and Oceanography*, *36*(3), 424–432. https://doi.org/10.4319/lo.1991.36.3.0424

Krom, M. D., Woodward, E. M. S., Herut, B., Kress, N., Carbo, P., Mantoura, R. F. C., Spyres, G., Thingstad, T. F., Wassmann, P., Wexels-Riser, C., Kitidis, V., Law, C. S., & Zodiatis, G. (2005). Nutrient cycling in the south east Levantine basin of the eastern Mediterranean: Results from a phosphorus starved system. *Deep Sea Research Part II: Topical Studies in Oceanography*, *52*(22), 2879–2896. https://doi.org/10.1016/j.dsr2.2005.08.009

LeGrande, A. N., & Schmidt, G. A. (2006). Global gridded data set of the oxygen isotopic composition in seawater. *Geophysical Research Letters*, *33*(12). https://doi.org/10.1029/2006GL026011

Lehmann, M. F., Sigman, D. M., & Berelson, W. M. (2004). Coupling the 15N/14N and 18O/16O of nitrate as a constraint on benthic nitrogen cycling. *Marine Chemistry*, *88*(1), 1–20. https://doi.org/10.1016/j.marchem.2004.02.001

Lehmann, M. F., Sigman, D. M., McCorkle, D. C., Granger, J., Hoffmann, S., Cane, G., & Brunelle, B. G. (2007). The distribution of nitrate 15N/14N in marine sediments and the impact of benthic nitrogen loss on the isotopic composition of oceanic nitrate. *Geochimica et Cosmochimica Acta*, *71*(22), 5384–5404. https://doi.org/10.1016/j.gca.2007.07.025

Mara, P., Mihalopoulos, N., Gogou, A., Daehnke, K., Schlarbaum, T., Emeis, K.-C., & Krom, M. (2009). Isotopic composition of nitrate in wet and dry atmospheric deposition on Crete in the eastern Mediterranean Sea. *Global Biogeochemical Cycles*, *23*(4). https://doi.org/10.1029/2008GB003395

Marconi, D., Alexandra Weigand, M., Rafter, P. A., McIlvin, M. R., Forbes, M., Casciotti, K. L., & Sigman, D. M. (2015). Nitrate isotope distributions on the US GEOTRACES North Atlantic cross-basin section: Signals of polar nitrate sources and low latitude nitrogen cycling. *Marine Chemistry*, *177*, 143–156. https://doi.org/10.1016/j.marchem.2015.06.007

Marconi, D., Weigand, M. A., & Sigman, D. M. (2019). Nitrate isotopic gradients in the North Atlantic Ocean and the nitrogen isotopic composition of sinking organic matter. *Deep Sea Research Part I: Oceanographic Research Papers*, *145*, 109–124. https://doi.org/10.1016/j.dsr.2019.01.010

Mariotti, A., Germon, J. C., Hubert, P., Kaiser, P., Letolle, R., Tardieux, A., & Tardieux, P. (1981). Experimental determination of nitrogen kinetic isotope fractionation: Some principles; illustration for the denitrification and nitrification processes. *Plant and Soil*, *62*(3), 413–430. https://doi.org/10.1007/BF02374138

Martínez-García, A., Jung, J., Ai, X. E., Sigman, D. M., Auderset, A., Duprey, N. N., Foreman, A., Fripiat, F., Leichliter, J., Lüdecke, T., Moretti, S., & Wald, T. (2022). Laboratory Assessment of the Impact of Chemical Oxidation, Mineral Dissolution, and Heating on the Nitrogen Isotopic Composition of Fossil-Bound Organic Matter. *Geochemistry, Geophysics, Geosystems*, *23*(8), e2022GC010396. https://doi.org/10.1029/2022GC010396

Martiny, A. C., Pham, C. T. A., Primeau, F. W., Vrugt, J. A., Moore, J. K., Levin, S. A., & Lomas, M. W. (2013). Strong latitudinal patterns in the elemental ratios of marine plankton and organic matter. *Nature Geoscience*, *6*(4), Article 4. https://doi.org/10.1038/ngeo1757

Mayer, B., Boyer, E. W., Goodale, C., Jaworski, N. A., van Breemen, N., Howarth, R. W., Seitzinger, S., Billen, G., Lajtha, K., Nadelhoffer, K., Van Dam, D., Hetling, L. J., Nosal, M., & Paustian, K. (2002). Sources of nitrate in rivers draining sixteen watersheds in the northeastern U.S.: Isotopic constraints. *Biogeochemistry*, *57*(1), 171–197. https://doi.org/10.1023/A:1015744002496

McRose, D. L., Lee, A., Kopf, S. H., Baars, O., Kraepiel, A. M. L., Sigman, D. M., Morel, F. M. M., & Zhang, X. (2019). Effect of iron limitation on the isotopic composition of cellular and released fixed nitrogen in Azotobacter vinelandii. *Geochimica et Cosmochimica Acta*, *244*, 12–23. https://doi.org/10.1016/j.gca.2018.09.023

Minagawa, M., & Wada, E. (1986). Nitrogen isotope ratios of red tide organisms in the East China Sea: A characterization of biological nitrogen fixation. *Marine Chemistry*, *19*(3), 245–259. https://doi.org/10.1016/0304-4203(86)90026-5

Pantoja, S., Repeta, D. J., Sachs, J. P., & Sigman, D. M. (2002). Stable isotope constraints on the nitrogen cycle of the Mediterranean Sea water column. *Deep Sea Research Part I: Oceanographic Research Papers*, *49*(9), 1609–1621. https://doi.org/10.1016/S0967-0637(02)00066-3

Powley, H. R., Krom, M. D., Emeis, K.-C., & Van Cappellen, P. (2014). A biogeochemical model for phosphorus and nitrogen cycling in the Eastern Mediterranean Sea: Part 2. Response of nutrient cycles and primary production to anthropogenic forcing: 1950–2000. *Journal of Marine Systems*, *139*, 420–432. https://doi.org/10.1016/j.jmarsys.2014.08.017

Powley, H. R., Krom, M. D., & Van Cappellen, P. (2017). Understanding the unique biogeochemistry of the Mediterranean Sea: Insights from a coupled phosphorus and nitrogen model. *Global Biogeochemical Cycles*, *31*(6), 1010–1031. https://doi.org/10.1002/2017GB005648

Pujo-Pay, M., Conan, P., Oriol, L., Cornet-Barthaux, V., Falco, C., Ghiglione, J.-F., Goyet, C., Moutin, T., & Prieur, L. (2011). Integrated survey of elemental stoichiometry (C, N, P) from the western to eastern Mediterranean Sea. *Biogeosciences*, *8*(4), 883–899. https://doi.org/10.5194/bg-8-883-2011

Pytkowicx, R. M. (1971). On the Apparent Oxygen Utilization and the Preformed Phosphate in the Oceans1. *Limnology and Oceanography*, *16*(1), 39–42. https://doi.org/10.4319/lo.1971.16.1.0039

Rafter, P. A., DiFiore, P. J., & Sigman, D. M. (2013). Coupled nitrate nitrogen and oxygen isotopes and organic matter remineralization in the Southern and Pacific Oceans. *Journal of Geophysical Research: Oceans*, *118*(10), 4781–4794. https://doi.org/10.1002/jgrc.20316

Rahav, E., Herut, B., Levi, A., Mulholland, M. R., & Berman-Frank, I. (2013). Springtime contribution of dinitrogen fixation to primary production across the Mediterranean Sea. *Ocean Science*, *9*(3), 489–498. https://doi.org/10.5194/os-9-489-2013

Redfield, A. C., Ketchum, B. H., & Richards, F. A. (1963). The influence of organisms on the composition of sea-water. *The Sea: Ideas and Observations on Progress in the Study of the Seas*. https://www.vliz.be/en/imis?module=ref&refid=28944&printversion=1&dropIMIStitle=1

Ren, H., Sigman, D. M., Meckler, A. N., Plessen, B., Robinson, R. S., Rosenthal, Y., & Haug, G. H. (2009). Foraminiferal Isotope Evidence of Reduced Nitrogen Fixation in the Ice Age Atlantic Ocean. *Science*, *323*(5911), 244–248. https://doi.org/10.1126/science.1165787

Ribera d'Alcalà, M., Civitarese, G., Conversano, F., & Lavezza, R. (2003). Nutrient ratios and fluxes hint at overlooked processes in the Mediterranean Sea. *Journal of Geophysical Research: Oceans*, *108*(C9). https://doi.org/10.1029/2002JC001650

Ridame, C., Dinasquet, J., Hallstrøm, S., Bigeard, E., Riemann, L., Van Wambeke, F., Bressac, M., Pulido-Villena, E., Taillandier, V., Gazeau, F., Tovar-Sanchez, A., Baudoux, A.-C., & Guieu, C. (2022). N_2 fixation in the Mediterranean Sea related to the composition of the diazotrophic community and impact of dust under present and future environmental conditions. *Biogeosciences*, *19*(2), 415–435. https://doi.org/10.5194/bg-19-415-2022

Sachs, J. P., & Repeta, D. J. (1999). Oligotrophy and Nitrogen Fixation During Eastern Mediterranean Sapropel Events. *Science*, *286*(5449), 2485–2488. https://doi.org/10.1126/science.286.5449.2485

Sanchez-Cabeza, J. A., Ortega, M., Merino, J., & Masqué, P. (2002). Long-term box modelling of 137Cs in the Mediterranean Sea. *Journal of Marine Systems*, *33–34*, 457–472. https://doi.org/10.1016/S0924-7963(02)00071-4

Sandroni, V., Raimbault, P., Migon, C., Garcia, N., & Gouze, E. (2007). Dry atmospheric deposition and diazotrophy as sources of new nitrogen to northwestern Mediterranean oligotrophic surface waters. *Deep Sea Research Part I: Oceanographic Research Papers*, *54*(11), 1859–1870. https://doi.org/10.1016/j.dsr.2007.08.004

Schneider, A., Tanhua, T., Roether, W., & Steinfeldt, R. (2014). Changes in ventilation of the Mediterranean Sea during the past 25 year. *Ocean Science*, *10*(1), 1–16. https://doi.org/10.5194/os-10-1-2014

Sigman, D. M., Altabet, M. A., McCorkle, D. C., Francois, R., & Fischer, G. (1999). The δ15N of nitrate in the southern ocean: Consumption of nitrate in surface waters. *Global Biogeochemical Cycles*, *13*(4), 1149–1166. https://doi.org/10.1029/1999GB900038

Sigman, D. M., Altabet, M. A., McCorkle, D. C., Francois, R., & Fischer, G. (2000). The δ15N of nitrate in the Southern Ocean: Nitrogen cycling and circulation in the ocean interior. *Journal of Geophysical Research: Oceans*, *105*(C8), 19599–19614. https://doi.org/10.1029/2000JC000265

Sigman, D. M., Casciotti, K. L., Andreani, M., Barford, C., Galanter, M., & Böhlke, J. K. (2001). A Bacterial Method for the Nitrogen Isotopic Analysis of Nitrate in Seawater and Freshwater. *Analytical Chemistry*, *73*(17), 4145–4153. https://doi.org/10.1021/ac010088e

Sigman, D. M., DiFiore, P. J., Hain, M. P., Deutsch, C., Wang, Y., Karl, D. M., Knapp, A. N., Lehmann, M. F., & Pantoja, S. (2009). The dual isotopes of deep nitrate as a constraint on the cycle and budget of oceanic fixed nitrogen. *Deep Sea Research Part I: Oceanographic Research Papers*, *56*(9), 1419–1439. https://doi.org/10.1016/j.dsr.2009.04.007

Sisma-Ventura, G., Bialik, O. M., Makovsky, Y., Rahav, E., Ozer, T., Kanari, M., Marmen, S., Belkin, N., Guy-Haim, T., Antler, G., Herut, B., & Rubin-Blum, M. (2022). Cold seeps alter the near-bottom biogeochemistry in the ultraoligotrophic Southeastern Mediterranean Sea. *Deep Sea Research Part I: Oceanographic Research Papers*, *183*, 103744. https://doi.org/10.1016/j.dsr.2022.103744

Smart, S. M., Ren, H., Fawcett, S. E., Schiebel, R., Conte, M., Rafter, P. A., Ellis, K. K., Weigand, M. A., Oleynik, S., Haug, G. H., & Sigman, D. M. (2018). Ground-truthing the planktic foraminifer-bound nitrogen isotope paleo-proxy in the Sargasso Sea. *Geochimica et Cosmochimica Acta*, *235*, 463–482. https://doi.org/10.1016/j.gca.2018.05.023

Tsimplis, M. N., & Bryden, H. L. (2000). Estimation of the transports through the Strait of Gibraltar. *Deep Sea Research Part I: Oceanographic Research Papers*, *47*(12), 2219–2242. https://doi.org/10.1016/S0967-0637(00)00024-8

Wang, X. T., Prokopenko, M. G., Sigman, D. M., Adkins, J. F., Robinson, L. F., Ren, H., Oleynik, S., Williams, B., & Haug, G. H. (2014). Isotopic composition of carbonate-bound organic nitrogen in deep-sea scleractinian corals: A new window into past biogeochemical change. *Earth and Planetary Science Letters*, *400*, 243–250. https://doi.org/10.1016/j.epsl.2014.05.048

Weigand, M. A., Foriel, J., Barnett, B., Oleynik, S., & Sigman, D. M. (2016). Updates to instrumentation and protocols for isotopic analysis of nitrate by the denitrifier method. *Rapid Communications in Mass Spectrometry*, *30*(12), 1365–1383. https://doi.org/10.1002/rcm.7570

Yogev, T., Rahav, E., Bar-Zeev, E., Man-Aharonovich, D., Stambler, N., Kress, N., Béjà, O., Mulholland, M. R., Herut, B., & Berman-Frank, I. (2011). Is dinitrogen fixation significant in the Levantine Basin, East

Mediterranean Sea? *Environmental Microbiology*, *13*(4), 854–871. https://doi.org/10.1111/j.1462-2920.2010.02402.x

Zhang, R., Wang, X. T., Ren, H., Huang, J., Chen, M., & Sigman, D. M. (2020). Dissolved Organic Nitrogen Cycling in the South China Sea From an Isotopic Perspective. *Global Biogeochemical Cycles*, *34*(12), e2020GB006551. https://doi.org/10.1029/2020GB006551

Global Biogeochemical Cycles

Supporting Information for

Origins of the nitrate ^{15}N depletion in the Mediterranean Sea

T. Wald[*1,2], F. Fripiat[3], A.D. Foreman[1], T. Tanhua[4], G. Sisma-Ventura[5], Y. Ryu[6], D. Marconi[6], D.M. Sigman[6], G.H. Haug[1,2], and A. Martínez-García[*1]

[1]Max Planck Institute for Chemistry, Mainz, Germany.

[2]ETH Zürich, Zürich, Switzerland.

[3]Department of Geosciences, Environment and Society, Université Libre de Bruxelles, Bruxelles, Belgium.

[4]GEOMAR Helmholtz Centre for Ocean research Kiel, Kiel, Germany.

[5]Israel Oceanographic and Limnological Research Institute, Haifa, Israel.

[6]Department of Geosciences, Princeton University, Princeton, NJ, USA

Contents of this file

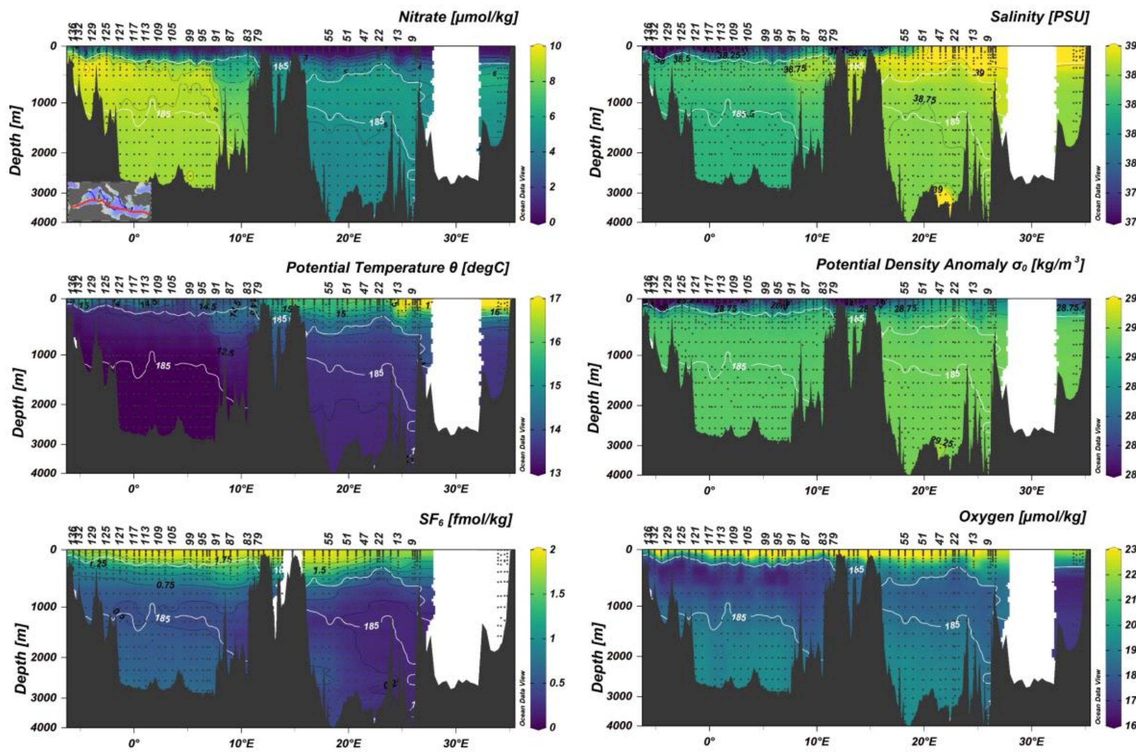

Figure S1. Physical properties in reference to the nitrate concentration of the zonal transect through the Mediterranean Sea. The white contour line indicates O_2 concentrations ≤ 185 µM, which is used to define the intermediate water mass.

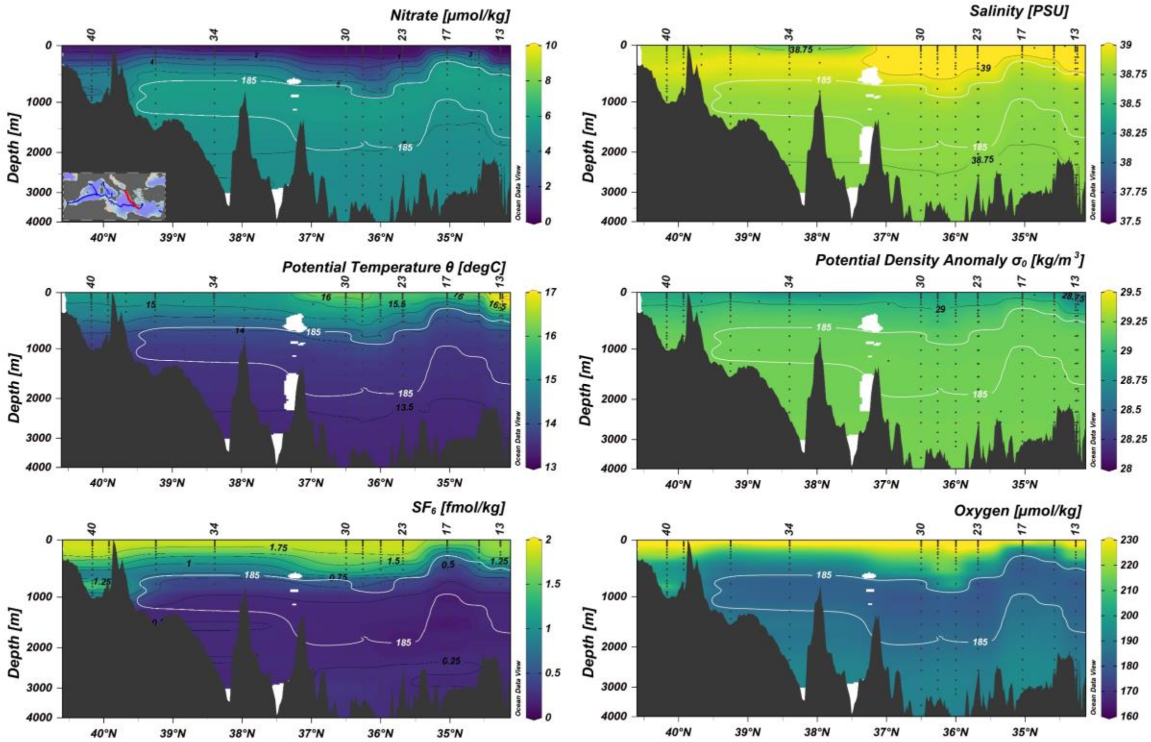

Figure S2. Physical properties in reference to the nitrate concentration of the Ionian section. Nitrate concentration, S, θ and σ_0 are comparable to the ones from the eastern basin. The white contour line indicates O_2 concentrations ≤ 185 µM, which is used to define the intermediate water mass.

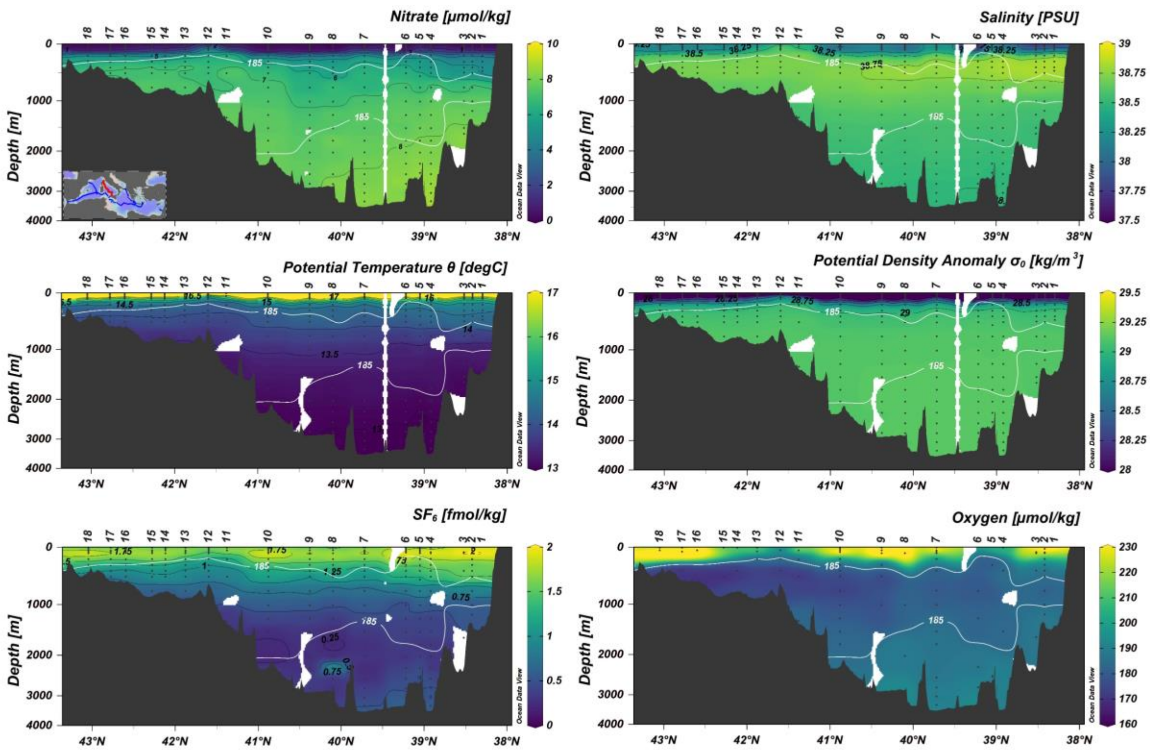

Figure S3. Physical properties in reference to the nitrate concentration of the Tyrrhenian section. Nitrate concentration, S, θ and σ_0 are comparable to the ones from the zonal transect between MSM72 stn. 75–91 of the western basin. The white contour line indicates O_2 concentrations ≤ 185 µM, which is used to define the intermediate water mass.

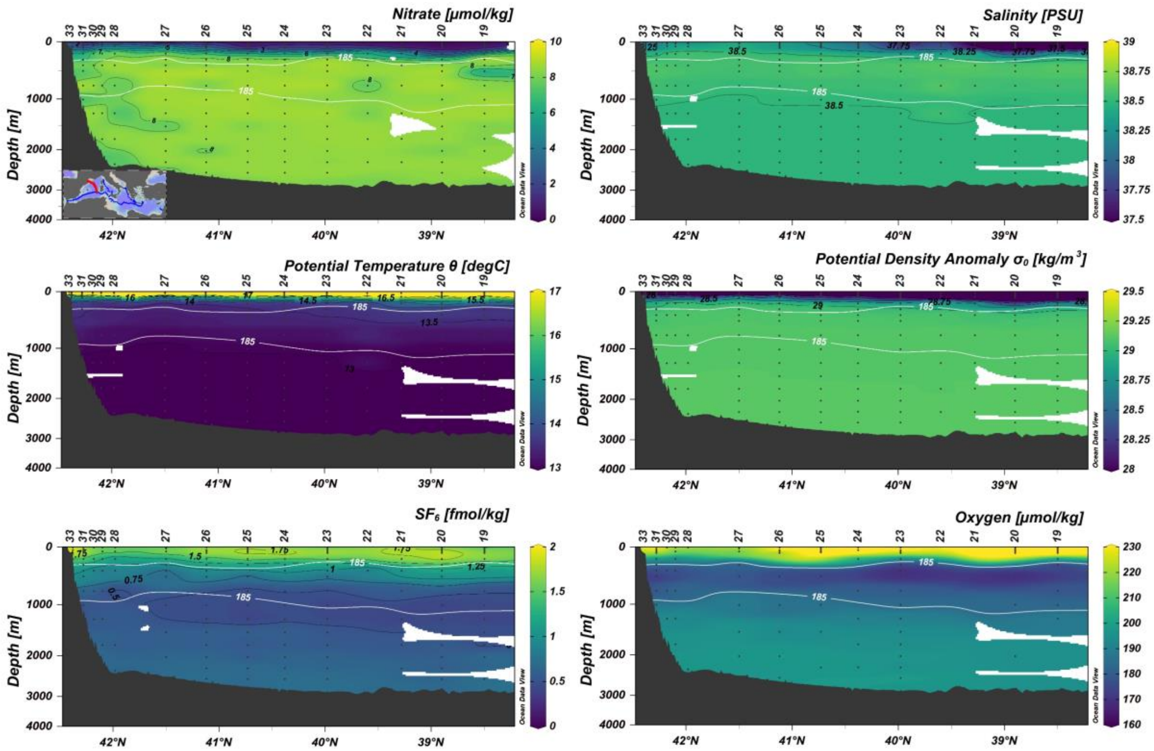

Figure S4. Physical properties in reference to the nitrate concentration of the Algerian section. Nitrate concentration, S, θ and σ_0 are comparable to the ones from the zonal transect between MSM72 stn. 93–136 of the western basin. The white contour line indicates O_2 concentrations ≤ 185 µM, which is used to define the intermediate water mass.

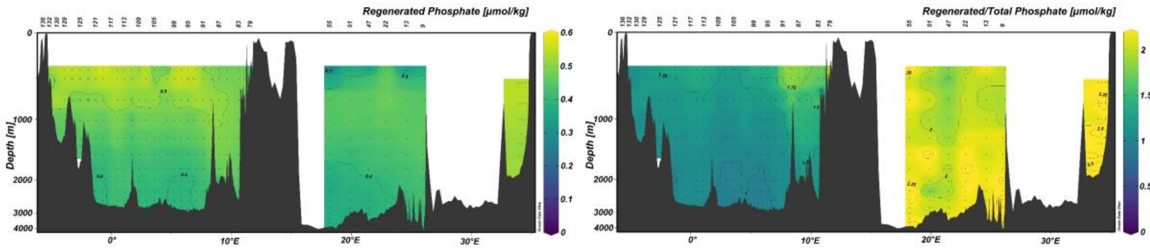

Figure S5. Regenerated phosphate and regenerated/total phosphate calculated with the Redfield stoichiometric ratios along the zonal transect.

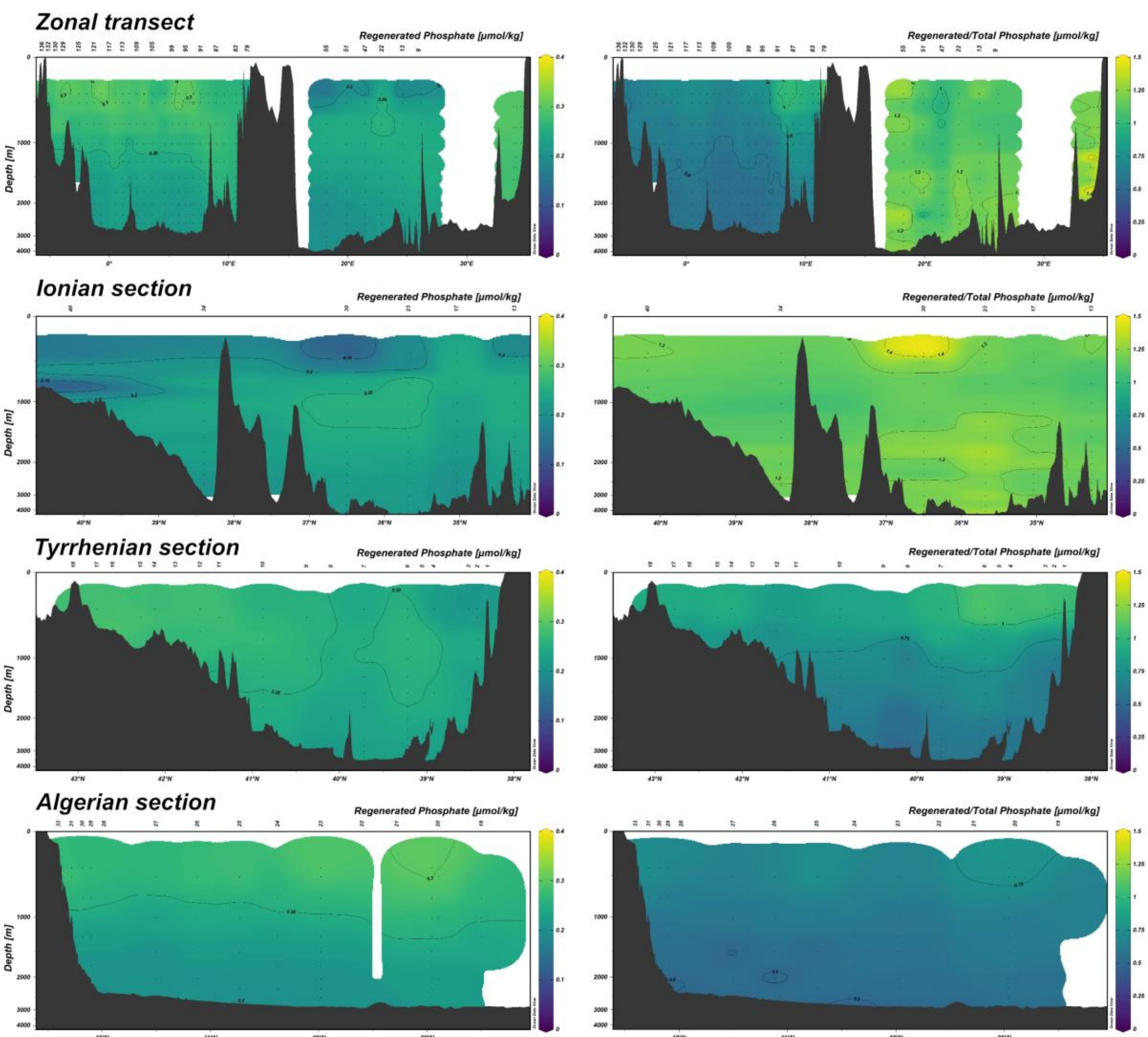

Figure S6. Estimation of the regenerated phosphate in each basin (left panels) and fraction of regenerated/total phosphate pool.

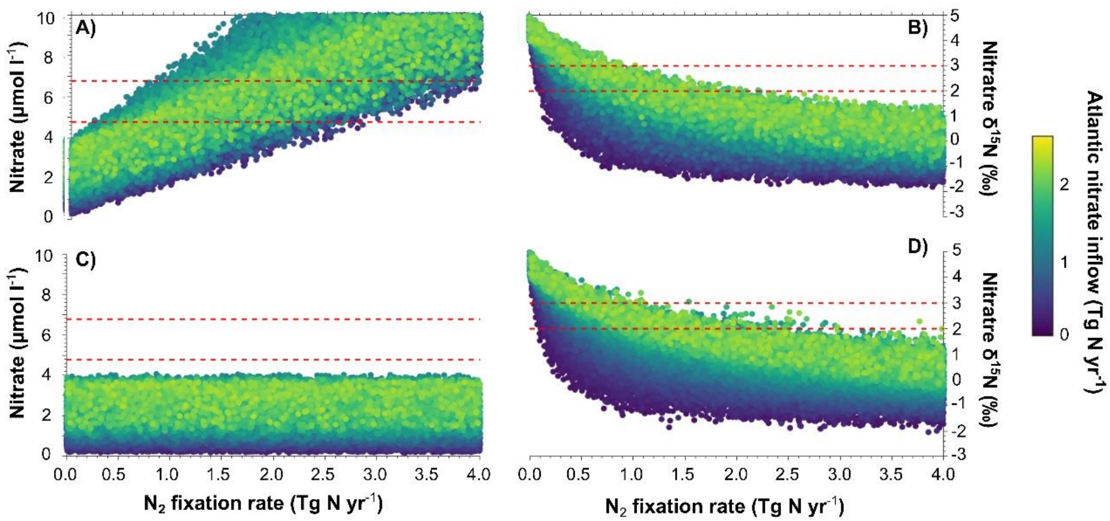

Figure S7. Model estimates of nitrate concentration (A, C) and nitrate $\delta^{15}N$ (B, D) in function of the N_2 fixation rate (in Tg N yr^{-1}) and nitrate supply from the Atlantic Ocean (color scale in Tg N yr^{-1}). Estimates for N_2 fixation without (A, B) and with sedimentary denitrification (C, D).